UNIVERSITÀ DEGLI STUDI DI PADOVA

FACOLTÀ DI INGEGNERIA

DIPARTIMENTO DI PRINCIPI E IMPIANTI DI INGEGNERIA CHIMICA "I. Sorgato"

TESI DI LAUREA IN INGEGNERIA CHIMICA E DEI PROCESSI INDUSTRIALI

CONTACT DRYING OF PARTICULATE PHARMACEUTICALS: MODELLING AND SIMULATION

Relatore: Prof. Paolo Canu

Correlatore: Prof. Joaquin Martinez

Laureando: MARCO INTELVI

ANNO ACCADEMICO 2009 – 2010

In memory of my father,
to the love of my mother

Summary

In order to give a concrete response to the need of predictive contact drying simulation tools in pharmaceutical industry, simulation programs for contact drying of pharmaceutical powders were developed in this thesis work. These are two programs for simulate the two main contact drying operation conditions used in the pharmaceutical industry: vacuum and atmospheric contact drying of agitated beds. The programs give a predictive estimation of drying rate curve and bulk bed temperature during contact drying. Only initial conditions, operating conditions, geometrical data, type of substances, solid phase properties and two parameter for the evaluation of an empirical mixing coefficient, are required as input data.

Each program consist in a main program for contact drying simulation, based on "Penetration theory". Several programs are used for evaluating: heat and mass transfer coefficients, effective particulate bed properties, physical and thermodynamic properties of gas and liquid phases. All these values are calculated several times along the process simulation, as function of the actual value of bed temperature and bed moisture content. The models used in these programs are choosen from literature as the most suitable for the simulation purpose and adapted to the scope of the work.

A first validation of the developed programs was made on experimental data from literature, regarding two common pharmaceutical excipient powders, wetted with water and dried in a disc contact dryer. The simulation results show a good agreement with the experimental data. Few deviation was identified, and a delimitation of the prediction limit of the used models is proposed.

Then, the programs give a predictive and accurate insight of the drying behaviour of the analyzed powders. With further validation on other substances and on industrial scale, the developed programs would be an useful tool for design, analysis, optimization and control of industrial contact dryers.

Riassunto

Nel presente lavoro di tesi sono stati sviluppati programmi di simulazione del processo di essiccamento a contatto di polveri farmaceutiche, al fine di dare una risposta concreta alla necessità di strumenti di simulazione predittivi nell'industria farmaceutica. Si tratta di due programmi per simulare le due più comuni operazioni di essiccamento nell'industria farmaceutica: essiccamento a contatto sotto vuoto e a pressione atmosferica di letti agitati. I programmi forniscono una stima predittiva delle curve di essiccamento e della temperature di bulk del letto. Sono richiesti come input ai programmi solamente le condizioni iniziali, condizioni operative, geometria del sistema, tipologia di sostanze coinvolte, proprietà della fase solida e due parametri per la valutazione di un coefficiente di mescolamento.

Ognuno dei programmi consiste in un programma principale di simulazione basato sulla "Teoria della penetrazione". Diversi programmi sono inoltre utilizzati per valutare: coefficienti di trasporto di materia e calore, proprietà effettive del letto, proprietà fisiche e termodinamiche della fase gas e della fase liquida.

Tutti questi valori sono calcolati varie volte durante la simulazione del processo, in funzione dei valori attuali di temperature e di umidità del letto. Tutti i modelli utilizzati provengono da letteratura e sono stati scelti come i più adatti agli obbiettivi di simulazione preposti e opportunamente adattati allo scopo del lavoro.

I programmi sviluppati sono stati validati su dati sperimentali di letteratura, riguardanti due comuni eccipienti farmaceutici in presenza di acqua ed essiccati in un essiccatore agitato a disco. I risultati delle simulazioni evidenziano una buona corrispondenza con i dati sperimentali. Alcune deviazioni sono state identificate, e quindi dei limiti nell'applicabilità dei modelli utilizzati vengono proposte.

I programmi forniscono un'accurata e predittiva stima del processo di essiccamento delle polveri analizzate. Con ulteriori validazioni su altre sostanze e su scala industriale, tali programmi potrebbero essere uno strumento utile per la progettazione, analisi, ottimizzazione e controllo degli essiccatori a contatto industriali.

Table of content

Chapter 1

Introduction

The present Master thesis work was carried out at the “Department of Chemical Engineering and Technology” of “Royal Institute of Technology – KTH” in Stockholm, Sweden. Inside this department, and inside the “Division of transport phenomena” there is the “Drying research group” directed by Prof. Joaquin Martinez. At this group, the thesis work was developed from March to September 2010, with the supervision of Prof. Martinez and Apolinar Picado.

1.1. Background

Many pharmaceutical products are distributed in solid form, like tablets, capsule, dragees or powder. It is important that the residual moisture content of the product is low enough to avoid product deterioration during storage and ensure free-flowing properties during the manufactory process, and during use. For this purpose, at the end of the manufacture of the dosage forms, usually following a crystallization step, the products are dried before packing. Also at the end of each intermediate stage of pharmaceuticals production that involves solids, the material is dried. Drying of pharmaceutical is one of the most sophisticated and expensive process in drying technology, because pharmaceuticals are often heat sensitive materials, oxidation of the product can take place in presence of normal atmosphere, and the contamination of the product must be severely avoid. Then, particular technology must to be used. For this scope *contact drying* and in particular *vacuum contact drying* are widely used to dry pharmaceutical granular material. (Aulton, 2007) (Mujumdar, 2007)

1.2. Motivation

A survey carried out among eleven of the mayor European chemical and pharmaceutical companies (Salangen, 2000) indicated that more research in drying technology is needed in this industrial sector. Most of the companies are not satisfy with their models for simulation of drying process, and they have highlighted a need to improve the applicability of contact drying models. Then, more research is wanted by the chemical and pharmaceutical companies from universities, and one of the first application where research is required is contact drying. Concerning contact drying, more research about the prediction of heat transfer coefficient and the effect of stirring has emerged. Also in the most recent publications about drying R&D, the need of research in drying appear as an open problem. More recently Prof. Arun S. Mujumdar says: ”Some 60’000 products need to be dried at different scales in over 100 dryers. The need of R&D is therefore enormous.” The need of mathematical model as predictive as possible, is also mentioned by Mujumdar. (Mujumdar, 2007)

1.3. Objective

The purpose of this work is the elaboration, and a first validation, of computer programs that can give a reliable simulation of the industrial contact drying of pharmaceutical powders, under several operating conditions. These programs would be an useful tool for design, analysis, optimization and control of industrial contact dryers.

For this aim, the program should make an estimation of drying rate curves and bed temperatures in contact drying of particulate pharmaceuticals. The prediction should be as predictive a possible, then only the operation condition, geometrical data, the type of the substances and a reduced number of parameter is required. All the physical and thermodynamic properties, all the effective properties and the mass/thermal coefficients should be compute with the more appropriate models available in literature.

The possibility to simulate all the typical contact drying operating conditions, used in the pharmaceutical industry, is an important focus of the work. For this reason two different programs are required, in order to simulate vacuum as well as normal pressure operation.

1.4. Thesis statement

In this writing, the Master thesis work carry out in order to reach the objective exposed before and the results obtained, are exposed. The structure of the thesis reflect the temporal sequence of the work.

The first part of the work coincides with chapter 2 and 3. In this part a study of the general aspect of drying theory was made. Chapter 2 is a qualitative presentation of the drying technology, with particular regards to contact drying process. In chapter 3 the main aspect of contact drying theory are reported. The transport phenomena that occur, i.e. heat and mass transfer, are analyzed during the drying process. Most of the theory exposed in this two chapter is the results of an analysis and re-elaboration of the chapters 1, 3, 4 and 6 of Mujumdar's Handbook of Industrial Drying (Mujumdar, 2007).

The second part of the work is described in chapter 4. In this part a literature review regarding the most important models for contact drying simulation, published from 1974 to present was made. This review regard most of the application of contact drying of particulate powders: packed beds, agitated beds, vacuum operation and normal pressure operations. In chapter 4 the models that will used later in the work are described in detail, the other models are shortly exposed with literature reference for further studies. In the last section of the chapter the motivation about the selection of the contact drying modelling techniques for agitated beds, used in the work, are explained. Also some advice for choosing a suitable model for packed bed contact drying are presented.

The third part is the modelling work, and coincides with chapter 5. A contact drying simulation model was build up for each one of two applications (vacuum contact drying of agitated beds and atmospheric contact drying of agitated beds), by using the most suitable models for heat/mass coefficients, effective properties, physical and thermodynamic properties. In chapter 5 the structure of the model and all the equations are specified. The sub-models are also described and the detailed equations are reported in the appendixes.

In the fourth part of the work the simulation programs of each one application are developed by using the software MATLAB®. In chapter 6 the structure of the programs, the cycle structure, the analysis of the required input data are exposed.

The fifth part of the work regard the analysis of the simulation results and a first validation with experimental data. The relative chapter, the number seven, contains the simulation results (drying rate curves and temperature profiles) in the two operation conditions with an analysis of the profiles of the effective properties and the thermal coefficients during the process. After this analysis, for each process a comparison of the simulation results with experimental data from literature regarding two common pharmaceutical excipient is presented.

In chapter 8 the conclusion, the limitation and the further prospective of the work are exposed.

Chapter 2

Drying Technology

2.1. Drying process

Drying is the separation operation that converts a wet solid or semisolid feedstock in a dry solid product, by thermal removing of the volatile substances. Almost always in the industries there is the presence of solid matter, and in many cases the final product is solid. Moreover, in some industrial areas the moisture content of the final product is one of the most important quality parameter. For this reason, drying is ubiquitous unit operation found in many industries, and perhaps the oldest, most common and most diverse of chemical engineering unit operations. (Mujumdar, 2007)

Drying of wet solids occurs by an heat supply, in order to vaporize the moisture content of the solid. Due to the high latent heat of vaporization and the many thermal resistances of the system, drying is one of the most energy intensive unit operations. Several studies report national consumption for industrial drying operation ranging from 10-15% to 20-25% in developed countries. Then a substantial amount of research is carry out in an attempt to minimize the energy consumption of the drying operations. (Mujumdar, 2007)

Drying is still an essential unit operation in the industry in order to obtained specific characteristics in the solid final product or intermediate, typical of the dry matter like: easy-handle, free flowing powder, preservation and storage, weight loss and the reduction in the transports cost, major quality of the product. In many process, an excessive moisture content may lead to irreversible damage to product quality and hence a non-saleable product. The typical industrial areas for the industrial drying application are: chemical, agricultural, biotechnology, food, polymer, ceramics, pharmaceutical, pulp and paper, mineral processing and wood process industry. Particular attention must be taken to the drying of some pharmaceutical, biological and

food product, because most of them are heat sensitive. An excessive drying of this product can induce an irreversible damage, loss of the biological activity and change of flavour and taste in the foodstuff. Other frequent problems related to an excessive drying are: colour change, chemical reaction and surface modification.

Heating mechanism

As mentioned before, drying is a widely diversified unit operation. For all the industrial areas and for all kind of applications where drying are involved, over 400 types of different dryers have been developed, and above 100 distinct types are now commonly available. (Mujumdar, 2007)

All of these dryers fall in two kind of drying process: *convective drying* and *contact drying*. The difference between the two processes is in how the energy is supply to the feedstock material: in the former the heat is supply by a hot gas flow and by an heated wall in the latter case. This difference has important consequences in the performance of the unit operation.

The convective drying (also known as direct drying) is probably the most common drying mode for particulate, sheet-form or pasty materials. Heat is supplied by convention between a heated gas flowing and the free surface of the solid. The evaporated moisture is carried away by the gas flow. For this purpose the most common gas used is: air, but inert gases, combustion gases or superheated steam are also used.

Contact or indirect drying, are more appropriate for specific application like in pharmaceutical industry or for very wet solids. The heat is supply through heated surfaces, and the heating of the wet material takes place mainly by conduction from this surface and then by conduction within the solid bed. The evaporated moisture is taking away by a low gas flow or by vacuum.

2.2. Contact drying

In contact (or indirect or conductive) drying the heating medium is not in contact with the product being dried. The heat source is a hot surface, and the wet material is in contact with it. The heat transfer to the material is mainly by conduction from this surface. A low gas flow or vacuum is used to carry out the evaporating moisture. The

solid material is usually mixed in order to eliminate the moisture gradient inside the bed.

In contact drying there are five elements: heat source, heat exchanging surface, wet particulate bed, a phase above the bed (or vacuum) and mixing device. In figure *2.1* an agitated bed contact drying equipment is choosen in order to shown these elements.

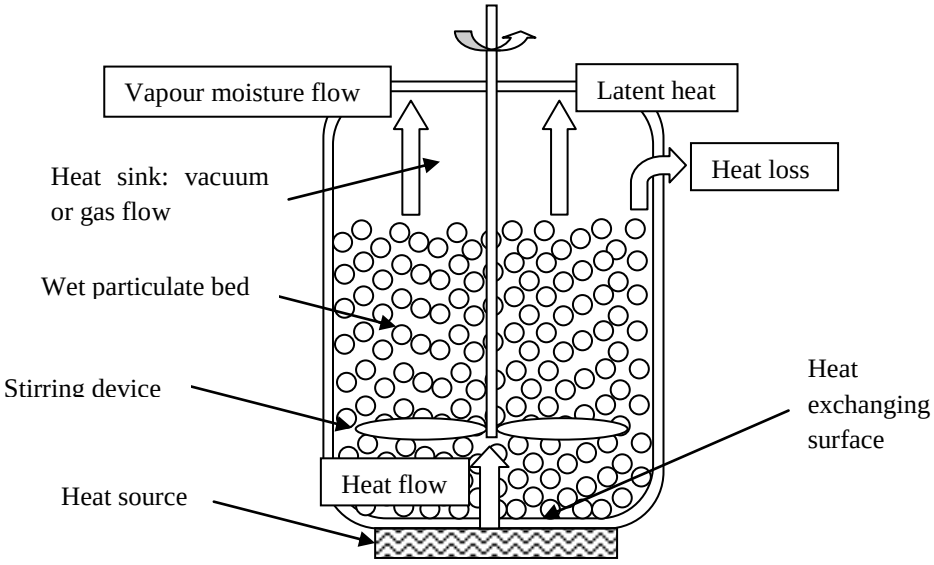

Figure 2.1. *Schematic diagram of an agitated bed contact dryer*.

The typical heat source use to heat the exchanging surface is: hot water steam, hot oil, molten salt, hot gas or combustion gas and electricity. The wet solid can take several different forms, from sheet to slurry, but the most common in pharmaceutical industry is the particulate form. For this reason the following treatment regarding in particular the contact drying of particulate matter. The phase above the solid is a gas phase or vacuum. Typical gases used in contact drying are or inert gases like Nitrogen. These gases are usually preheated to minimize localized condensation. The solid bed mixing is usually obtained by an agitator or by the rotation of the drying chamber.

Contact drying presents several advantages comparing to convective drying. Some of these are: higher energy efficiency (2’800 – 3’600 kJ/kg of water evaporated), waste heat source can be used, minimal cleaning of the exhaust gas, low emission of particulate matter from the dryer, higher product quality attainable, adapt when hygienic condition are required. For the vacuum contact drying there are also the advantage reported later in the section about “Operating pressure”. Accompanying the above

advantage there are several limitations: the heat flux is limited to the available hot surface area, many types of contact dryers can only be operate in batch mode, lower maximum drying temperature respect to the convective drying and typically high capital cost. (Mujumdar, 2007)

The application of contact drying is very wide: from several solid and powder foods, to chemicals, pharmaceuticals, pigment, clay and peat. There are different types of contact dryers, the most common for particulate material are: rotary dryers, rotating double cone dryer and agitated bed dryers. Anyhow the modelling of these different kind of dryers is very similar, the two main important characteristics that influence the drying performance and then the modelling of the contact drying equipment for powder are the operating pressure (vacuum or normal pressure) and the presence of stirring in the bed.

Operating pressure

Contrary to convective drying, contact drying can be operated both at normal pressure or under vacuum. For drying common materials that are not heat sensitive, normal pressure contact drying is normally used. But, as mentioned above, some material to be dried like pharmaceutical, biological and food product, are heat sensitive and particular attention must be taken to the product temperature during drying. In case of heat sensitive material, vacuum operation is ideal because of solvent vaporization taken place at lower temperature (respect to the normal boiling temperature of the moisture). Other advantage related to the vacuum operation is the almost complete absence of oxygen that can minimized or eliminate oxidative reactions, and prevention of fire or explosion risk.

Stirring

Stirring is a very influencing parameter in contact drying of particulate material. In the most of the case the product to being dried is mechanically stirred, by rotation of the dryer (rotary and double cone dryer) or by a stirring device inside the particle bed. The aim of the particle mixing during contact drying is the elimination of the temperature and moisture content gradients within the bed, in order to reach an uniform temperature and moisture content inside the bed; and in this way the drying rate is enhanced. Recently in some industrial application, included the pharmaceutical industry, static bed

contact drying, or more frequently intermittent stirring operation are used. A totally static bed or the presence of alternating static and mixing period are commonly used when the preservation of the initial particle dimension and shape are an important aim.

Chapter 3

Contact drying theory

In this chapter the basic theory concept concerning the thermodynamics and transport phenomena in contact drying are reported, in order to describe the main concept for the rest of the work. Several topics are common for both, convective and contact drying. In that case the term "drying" is used. Otherwise, if the topics are closely related to contact drying, it is specified by the term "contact drying".

3.1. Overview of thermodynamics

Drying process is based on vaporization of the wet solid moisture content. The typical quantification of the evaporation flux in drying technology is *drying rate* $\dot{m}$. That is the rate of moisture evaporated per unit of heating surface area:

$$\dot{m} = \frac{mass\ of\ evaporated\ moisture}{unit\ of\ time\ \times unit\ of\ surface} = \left[\frac{kg}{s \cdot m^2}\right] \tag{1}$$

Vaporization is an endothermic process that required an amount of energy per mass or mole unit, that is called respectively *mass or molar enthalpy of vaporization* Δh_{ev}. This value is a function of the liquid species and the temperature of the system. Then the drying rate is connect to the *heat flux of vaporization* $\dot{q}_{lat}$ by the following equation:

$$\dot{m} = \frac{\dot{q}_{lat}}{\Delta h_{ev}} \tag{2}$$

Vaporization of the moisture occurs if the vapour pressure of the moisture content of the solid at the operating temperature $P^0_{m\to s}(T_b)$, is equal o larger than the surrounding pressure P. In particular, if $P^0_{m\to s}(T_b) = P$, the system is just at thermodynamic equilibrium then T_b coincides with the saturation temperature $T_s(P)$. If $P^0_{m\to s}(T_b) > P$, the liquid loses its latent heat, until it reach the saturation temperature at the surrounding

pressure $T_s(P)$. Then, the thermodynamic equilibrium is reach anyway. These cases are typical in vacuum contact drying, where the surrounding pressure is usually lower enough to reach the moisture vapour pressure around room temperature. Then, in vacuum operation, vaporization occurs at lower temperature compared to other drying operations, and the particle bed can keep at "safety temperatures" for heat sensitive materials. For drying rate calculation, a heat balance must be solved in the dryer, in order to compute the latent heat flux available in the bed for the vaporization. Now, by eq. (2) the drying rate can be evaluated.

When the wet solid is taking in contact with a non saturated gas phase, the moisture vaporization can also occur although the vapour pressure of the moisture is less than the operating pressure. This phenomenon, usually called *evaporation*, in order to distinguee it from the former, take place by a mass transfer phenomenon, caused by a gradient between the vapour pressure of the moisture in the solid $P^0_{m\to s}(T_b)$ and the partial pressure of the moisture in the gas phase p_m^{gas}. This phenomenon usually occurs in convective drying and in contact atmospheric (normal pressure) drying. In this case, in order to reach high value of drying rate, a highest heating temperature is required compared to a vacuum operation. In other words, for an equal heating temperature, vacuum contact drying can give higher drying regime respect to normal pressure operation. In this case the drying rate is calculated directly. It is proportional to the pressure gradient driving force by a mass transfer coefficient. The latent heat required for the evaporation of the moisture can be calculated in a second time by eq. (2).

Bound and unbound moisture

There are two kind of moistures that can carry away during the drying: *bound moisture* and *unbound moisture*. Bound moisture is the moisture: in chemical combination with the solid, in chemical or physical adsorption on the surface of the solid, dissolved with the solid, in cellular structure, retained in the capillaries, or trapped in the microstructure of the solid. Unbound moisture is the moisture in excess of bound moisture. All the non-hygroscopic materials content only unbounded moisture; the hygroscopic one can content both. The drying behaviour of the two kind of moistures present some different topics discussed later.

3.2. Overview of transport phenomena

The drying process consists in the wet solid moisture removal. This occurs by moisture vaporization or evaporation as seen before, a series of moisture mass transfer phenomena from the core of the solid to the surrounding of the bed and a series of heat transfer phenomena from the heating source to the solid core. Then, when a wet solid is subjected to a contact drying process, two transport phenomena take place: energy transfer and mass transfer, and the two transport phenomena are closely related to each other. The analysis and modelling of contact dryers are made by the description of the heat and mass transfer phenomena that take place in the process. For this reason is important to understand all the transport mechanisms that are present. A description inspired to the one proposed by Schlünder and Mollekopf (Schlünder & Mollekopf, 1984), completed with some information from the Mujumdar's Handbook of Industrial Drying (Mujumdar, 2007) are presented.

Energy transfer

In contact drying, the heat supplies by the heating wall must reach the core of the single particles. In this process three energy transfer phenomena can be identified. The first is the heat transfer from the hot surface at temperature T_w to the surface of the first particle layer in contact with it at temperature T_H[1]. This is a complex interphase heat transfer that involves conduction in the gas gaps and at the contact point of the wall and the particles, and radiation.

The second phenomenon is the energy transfer through the particle bed, from the first particle layer to the bulk of the bed at temperature $T_b < T_H$. This is also a combination of heat transport mechanism: particle to particle conduction, conduction in the interparticle gas gaps and radiation. If the heat transport occur where the bed particles are still wet or partially wet, the effect of the conduction of the liquid phase inside and outside the particle pore, and the effect of the heat transfer by liquid evaporation, vapour diffusion and recondensation should be taken into account.

[1] The temperature at the hot wall in contact with the bed is assumed to be known, then the heat transfer description starts from here.

In conclusion, in order to reach the particle core, heat transfer from the particle surface to the bulk of the particle at temperature $T_p < T_b$ occur. The mechanism is conduction inside the solid and in the gas-filled particle pores. Also in this case, if the particles are still wet, the mechanism connected to the presence of a liquid phase inside the pore can enhance the thermal diffusivity inside the particles.

A qualitative representation of the temperature profile in the bed and in the particles with the relative temperature are shown in figure *3.1*.

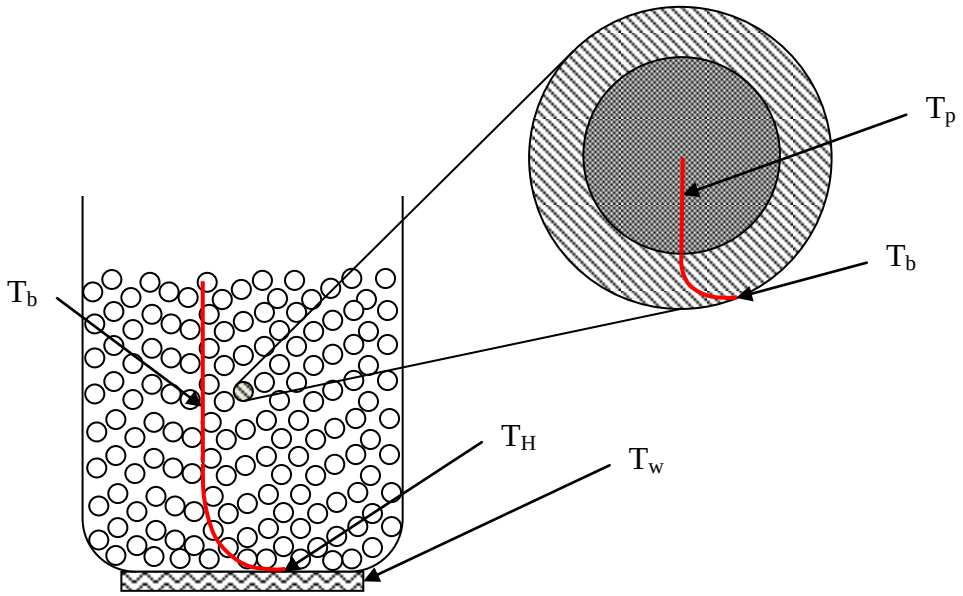

Figure 3.1. *Graphical representation of the temperatures used to describe the heat transfer phenomena in contact drying.*

Mass transfer

Regarding the moisture mass transfer from the core of the single particles to the surroundings, in the general case, there are three phenomena. In the first one, the liquid in the bulk of the particle migrate to the particle surface, and different transport mechanisms are involved. Transport of moisture within the solid may be occurring by: liquid diffusion, vapour diffusion, Knudsen diffusion, surface diffusion or hydrostatic pressure difference. The second phenomenon is the moisture penetration through the particulate bed. This transport occurs mainly by vapour diffusion in the interparticle gas gaps. Then, the vapour moisture that has reach the bed surface, pass from there to the

gas phase flow over the bed, by convection. This mass transport appears only in convective drying and atmospheric contact drying. It is absent in vacuum contact drying where there is no mass transfer resistance to carry away the moisture from the bed surface.

Mass transfer mechanism during constant rate period

During the drying process the moisture content of the wet solid is falling down and the dominant mass transfer mechanism, and then the drying behaviour of the feedstock, should be changed, and three different drying rate phase can be identified and shown in figure *3.2*.

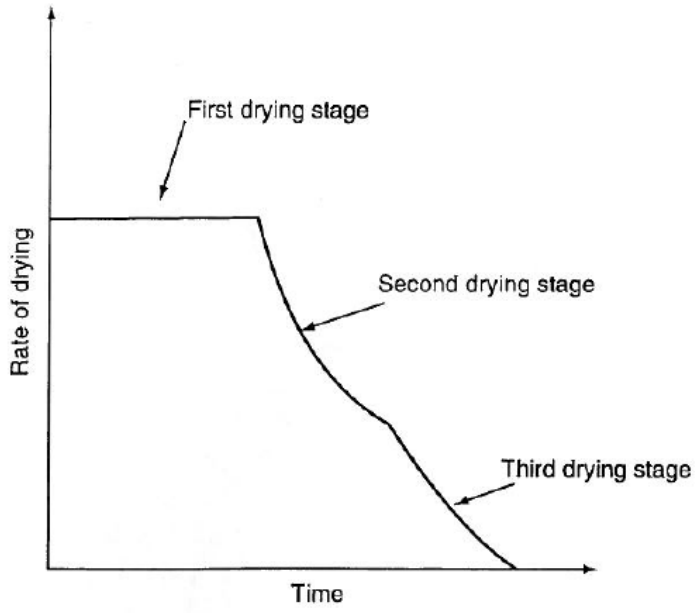

Figure 3.2. *Qualitative profile of drying rate during a general drying process. (Mujumdar, 2007)*

In the initial phase of the drying process the feedstock is totally wet, then its surface is completely covered by a liquid layer of unbound moisture, and the vaporization take place at the solid surface. This phenomenon is called *surface vaporization.* The behaviour of the *unbound* moisture of the layer around the solid is almost the same as the behaviour of pure isolated moisture. Then its vapour pressure $P_{u,m}^{0}(T_b)$ coincides with the vapour pressure of the pure and isolated moisture at the same temperature $P_{m}^{0}(T_b)$ and that value is constant at constant bed temperature:

$$P_{u,m}^{0}(T_b) = P_{m}^{0}(T_b)$$

In convective drying during this phase, if the bed temperature and the operating pressure are constant, and the moisture content of the gas phase is constant, the drying rate is also constant. For this reason the surface evaporation coincides with the so called *constant rate period* or *first drying stage*.

Due to the absence of particle and bed resistance, this constant value of the drying rate is also the maximum value of drying rate during the drying process and is called *maximum drying rate*.

Mass transfer mechanism during falling rate period

With the decreasing of the solid moisture content the surface area moisture layer start reduced by evaporation and dry spot appear upon the surface. The corresponding value of moisture content is called *critical moisture content*. If drying rate is computed with respect to the overall solid surface area, the drying rate fall even though the evaporation flux remains constant. This is the *first part of the falling rate period* or the *second drying stage*.

Where the unbound moisture layer at the solid surface is completely removed by drying, another mass transfer phenomenon is starting simultaneously: the mass transfer of interior bound moisture. In these areas the surface is dry but the interior of solid is still wet. Then a water concentration gradient appears, which produce a moisture migration from the bulk of the solid to the surface with the mechanism described before. When the whole surface of the solid is totally dry, the internal solid mass transfer probably could be the controlling mass transfer step. This further mass transfer resistance causes another fall down in the drying rate. This is the *second part of the falling rate period* or the *third drying stage*.

In vacuum contact drying description, if the particles to be dried are hygroscopic, since the critical moisture content is reach, the internal mass transfer should be taken into account like a further mass transfer resistance, by a modified bed heat capacity (Tsotsas & Schlünder, 1987) or by use experimental *characteristic drying rate curve* (Mujumdar, 2007).

Regarding normal pressure contact drying, as seen before, the moisture usually leave the solid by evaporation. Then the driving force of the process is the partial pressure gradient between the vapour pressure of *bound* moisture within the solid $P_{b,m}^{0}(T_b)$ and

the partial pressure of moisture in gas phase p_m^{gas}. But, the partial pressure of the moisture inside the solid (bound moisture) is not longer equal to the vapour pressure of the pure isolated liquid at the same temperature (like in the surface evaporation) but it is lower:

$$P_{b,m}^0(T_b) < P_m^0(T_b)$$

The lowering in the vapour pressure of moisture is the effect of the vaporization hindered, by the diffusivity resistance inside the solid, but also by moisture – solid bounding, moisture dissolving into the solid or mechanically blocked inside it, and the difficult to remove that is increasing during the drying. For this reason, as the internal moisture evaporation proceed, the vapour pressure of the moisture inside the solid fall down, and if the moisture content of the surroundings is constant, an equilibrium is reach. The solid moisture content at the equilibrium is called the *equilibrium moisture content* X^* and is a characteristic value of the wet product. It is a function of the operating conditions, and the gas phase moisture content. All the removable moisture, i.e. all the moisture that is removed until the critical moisture content, at a given operating condition is call *free moisture*.

In conclusion, regarding the vapour phase moisture within the solid, there is an additional vapour pressure gradient, as a result of a temperature gradient within the solid. This vapour pressure gradient (high vapour pressure inside the solid where the temperature is low, and low vapour pressure near the surface, where the temperature is high) generate an additional driving force to the mass transfer of moisture in the vapour phase from the bulk of the solid to the particle surface.

Chapter 4

Models for contact drying simulation: a review

Some different modelling techniques for contact drying simulation have been proposed in the last five decades and are available in literature. In this chapter a literature review about the most used and cited models for contact drying simulation is reported. In section *4.1* the models for transport phenomena in the bed (from the heating wall to the bulk of the bed) are described. In section *4.2* the particle modelling, i.e. the description of transport phenomena inside the single particle are exposed. A short review about the most recent modelling techniques in contact drying is presented in section *4.3*. In the last section: *4.4* the most suitable model for this Thesis work are choosen. For that scope some comparison between the models and remarks are presented.

4.1. Particulate bed modelling

At the beginning of the 70th, some works about heat transfer in particulate beds were published by Prof. Ernst Ulrich Schlünder and co-workers, in particular regarding:

- Heat transfer between heated flat plate and a particle layer in contact with it;
- Heat transfer across the particulate bed.

In the rest of this thesis work the two heat transport phenomena will be indicated respectively as: *contact heat transfer* and *heat penetration transfer*, following the Schlünder and co-workers nomenclature. The literature about the estimation of these two heat transfer coefficients and the application to contact drying modelling is presented below.

Contact heat transfer coefficient

As seen in the previous chapter, contact heat transfer coefficient between heating wall and the first particle layer is a complex phenomenon that involves the heat transfer at the "particle to wall" contact points, and through the gas gaps between the particles and the heating surface.

In 1971, Schlünder proposed a model for the prediction of heat transfer coefficient between an heated flat plate and a bed of particulate spherical material (Schlünder E. U., 1971). One of the first exposition in English of the model can be found in a subsequent publication (Schlünder E. , 1980). Later, some modifications of the original equations were published.

In this Thesis work the equation proposed by Schlünder in 1984 (Schlünder E. U., 1984) and summarized in other Schlünder work (Schlünder & Mollekopf, 1984) were used. In this model the contact heat transfer coefficients α_{ws} is estimated as a sum of three heat transport phenomena: conduction in the contact point α_{wp}, conduction in the gas-filled gaps α_{gaps} and radiative heat transfer α_r:

$$\alpha_{ws} = \phi_A \, \alpha_{wp} + (\phi_A - 1)\alpha_{gaps} + \alpha_r \qquad (3)$$

where ϕ_A is the *plate surface coverage factor*. The model developed by Schlünder is today one of the most used for prevision of contact resistance in drying simulation, and for this reason it was choosen for this work, and then it is exposed in detail in *Appendix A*.

Heat penetration coefficient

Heat transfer in dry beds

The first pubblication in English by Schlünder and co-workers about heat transfer in particlulate bed was made in 1974 (Wunschmann & Schlünder, 1974). In this work, models for prediction of heat transfer coefficient across a dry packed bed, as well as dry stirred bed of particulate material, under vacuum and normal pressure, were reported. The same models were described by Schlünder in 1980, one for packed bed and one for stirred bed (Schlünder E. , 1980).

In the *packed bed* model the bed is assumed as a continuum and the heat penetration coefficient α_{sb} is computed by Fourier theory of conduction. The solution is:

$$\alpha_{sb} = \frac{2}{\sqrt{\pi}} \sqrt{\frac{\left(\lambda/\rho\ c_p\right)_{dry,bed}}{t}} \tag{4}$$

where λ, ρ, c_p, are respectively the thermal conductivity, the density and the specific heat capacity referred to a dry packed bed, and t is the time coordinate. The limiting equation for fully developed temperature profile inside the bed is:

$$\lim_{t\to\infty} \alpha_{sb} = 3\ \frac{\lambda_{dry,bed}}{h} \tag{5}$$

where h is the high of the bed.

The model for *stirred bed* is based on the same assumption, and in order to taking into account the effect of particle mixing, the bed is assumed to be static for a certain contact time t_R. In this period the bed absorb heat like a static bed. After that, perfect mix of the bed is assumed. The heat transfer coefficient during the static period becomes:

$$\alpha_{sb} = \frac{2}{\sqrt{\pi}} \sqrt{\frac{\left(\lambda/\rho\ c_p\right)_{dry,bed}}{t_R}} \tag{6}$$

where t_R is a parameter called *contact time*. It can be estimated by correlation of experimental data as reported in the Schlünder of 1980. In the same work comparison between experimental and predicted data of penetration heat transfer coefficents were showed for packed and stirred beds. In the follow work by Schlünder (Schlünder E. U., 1984), other comparison between experimental and predicted data for penetration heat transfer coefficents showed a fairly well agree.

Heat transfer in wet beds under vacuum: Penetration theory

The heat transfer across particulate bed during contact drying takes place, at least in the early stage, in a wet bed. Then, in order to describe the contact drying process, models for heat transfer in wet particulate beds are required.

Schlünder and Mollekopf in 1984, starting from a previous work of Mollekopf (Mollekopf, 1983), and from the Schlünder and Wunschmann research about heat transfer in particulate beds exposed before, proposed the "*Penetration teory*" for the prediction of heat penetration coefficient in *stirred beds* during vacuum contact drying

(Schlünder & Mollekopf, 1984). This theory was developed in order to take into account the effect of the random particle motion, of a set of wet and dry particle, on the penetration heat transfer. It is based on a new physical view of the simultaneous mixing and drying process of a particulate bed. This continuous process is modelled by splitting in two sub-sequential periods:

- *Contact period* is a fictitious period during that the bed is static. There is the heat transfer penetration from the heating wall to the bulk of the bed. The heat penetration is described like the movement of a distinct heating front, parallel to the hot surface called *drying front*. The distance from the heating surface to the drying front is indicated as z_T. Between the heating surface and the drying front the particles are dry, and beyond that the particles are still wet. Between the heating surface and the drying front the particles are dry, and beyond that the particles are still wet. In the wet part of the bed the temperature is uniform and equal to the saturation temperature of the liquid at the operating pressure T_s. In the dry part of the bed a temperature profile exist between the heating wall at T_w and the drying front at T_s. The time length of this period is called *contact time* t_R.
- *Mixing period* is an instantaneous period that produces the perfect macro-mixing of the bed. Then, temperature and moisture content gradient disappeared in the bed and no transport phenomena occur.

The two periods are following each other. During every contact period the drying front penetration produce a drop in the bed moisture content and a bed temperature rise. With every following mixing period the front is eliminated and both, moisture content and temperature of the bed, are spatially equalized at the spatial mean value reach in the immediately preceding static period. A graphical representation of the sub-sequential period is shown in figure *4.1*.

Regarding the mathematical model, the particulate bed is assumed as a quasi-continuum and the heat penetration coefficient during the contact period, is calculated with the same approach used by Wunschmann and Schlünder (1974).

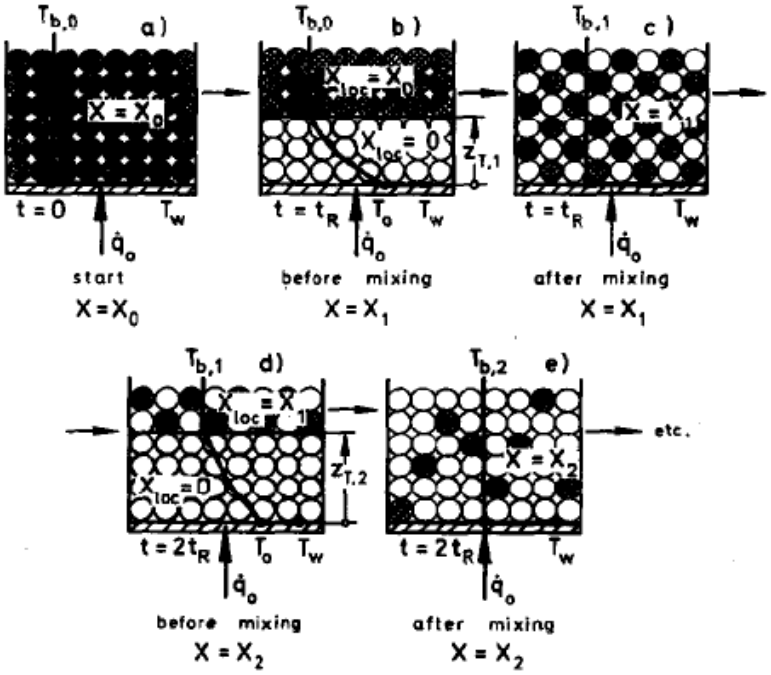

Figure 4.1. *Graphical representation of contact period and mixing period in penetration theory.* (Schlünder & Mollekopf, 1984)

Then, Fourier equation for heat transfer was integrated from the heating wall to the drying front[2]:

$$\left(\rho\, c_p\right)_{dry,bed} \frac{\partial T}{\partial t} = \lambda_{dry,bed} \frac{\partial^2 T}{\partial z^2} \tag{7}$$

with the following set of boundary conditions:

$$z = 0 \rightarrow T = T_H \tag{8}$$

$$z = z_T \rightarrow T = T_s \tag{9}$$

$$\rho\, X\, \Delta h_{ev} \frac{\partial z_T}{\partial t} = -\lambda_{dry,bed} \frac{\partial T}{\partial z} \tag{10}$$

The heat transfer coefficient across the bed, heat penetration coefficient, can be estimated from the temperature profile obtained by the resolution of eq.(7), the result is:

$$\alpha_{sb} = \frac{2}{\sqrt{\pi}} \sqrt{\frac{\left(\lambda/\rho\, c_p\right)_{dry,bed}}{t_R}} \frac{1}{erf\zeta} \tag{11}$$

[2] In this part of the bed the particles are assumed dry, for this reason the properties in the equations are referred to a dry bed.

where ζ is the *reduced position of drying front*. The calculation of ζ and some other detail about penetration theory are explained in *Appendix B*.

Regarding the contact time the authors of the penetration theory proposed to calculate it as a product of the time scale of the mixing, t_{mix} and an dimensionless parameter called *mixing number*, N_{mix} :

$$t_R = t_{mix}\, N_{mix} \tag{12}$$

The first term can be assumed equal to the inverse of the stirring frequency *f*, but for the second one, there is no theory for predict it. This parameter depends on the type of dryer and its stirring device, and it say: "how often the mixing device must have turned around before the product has been ideally mixed once" (Schlünder & Mollekopf, 1984). Only empirical correlation are available for N_{mix}.

The first empirical correlation for the prevision of the mixing number was proposed by Mollekopf (1983) for disc dryers:

$$N_{mix} = 4\, n^{-0.4} \tag{13}$$

Where n is the stirring frequency in round per minute. Another correlation was proposed by Schlünder and Mollekopf (1984) for disc, drum and paddle dryers:

$$N_{mix} = C\, Fr^{x} \tag{14}$$

where Fr is the *Froude number* defined as:

$$Fr = \frac{(2\,\pi\, n)^2 D}{2\, g} \tag{15}$$

C and x are two empirical parameter obtained by fitting on experimental drying rate curves. Value of these parameters for disc, drum and paddle dryers are reported by Schlünder and Mollekopf (1984).

For drying of a *packed bed* of particulate material, the concepts of Penetration theory could be applied, but in this case only contact periods occur, and a continuous penetration of the drying front is assumed to take place inside the bed (Mollekopf, 1983). Then, the equation for the heat penetration coefficient estimation became:

$$\alpha_{sb} = \frac{2}{\sqrt{\pi}} \sqrt{\frac{\left(\lambda/\rho\, c_p\right)_{dry,bed}}{t}}\, \frac{1}{erf\zeta} \tag{16}$$

where t is the time coordinate of the process. In this case no experimental coefficients are required, and the heat penetration coefficient can be calculated only from effective bed properties.

Heat transfer in wet beds at normal pressure

In 1986 Tsotsas and Schlünder proposed a model for the estimation of heat penetration coefficient in stirred bed, during drying process at normal pressure, inspired to Penetration theory (Tsotsas & Schlünder, 1986). The effects of random particle motion on heat transfer is described following Penetration theory, but no distinct drying front within the bed are assumed in this case, and the whole bed is assumed partially wet.

The solution of Fourier equation give the following expression for the heat penetration coefficient:

$$\alpha_{sb} = \frac{2}{\sqrt{\pi}} \sqrt{\frac{\left(\lambda/\rho\ c_p\right)_{wet,bed}}{t_R}} \tag{17}$$

Note that since the penetration heat transfer takes place through a *wet bed*, the effective bed properties in the calculation are referred to a wet bed condition. Contact time is estimated following the Penetration theory approach, and an empirical correlation for mixing number could be used.

Application to contact drying modelling

Vacuum contact drying

In 1984 Schlünder and Mollekopf gave the first complete description of contact drying modelling of stirred particulate material using Penetration teory (Schlünder & Mollekopf, 1984).

The contact drying modelling is referred to vacuum operation, and take into account the following transport phenomena:

- *Contact heat transfer*, i.e. heat transfer from the heating wall to the first particle layer (described by Schlünder model);
- *Heat penetration transfer*, i.e. heat transfer across the particulate bed (decribed by Penetration theory);

and these are assumed that they take place in series. No mass transfer resistance across the bed and no intrparticle mass transfer resistance are takeing into account. For the authors this kinds of transport resistances are negligible, compared to the contact and penetration heat transfer resitances, in particular compared to the second one, that seems to be the controlling heat transfer process along all the preocess[3].

Normal pressure contact drying

Regarding the application of penetration theory to contact drying at normal pressure, the first work is by Tsotsas and Schlünder (Tsotsas & Schlünder, 1986). In this case two more transport phenomena are taking into account, respect to the vacuum case:

- heat transfer of moisture from the free surface of the bed to the bulk of the adjacent gas phase;
- mass transfer of moisture from the free surface of the bed to the bulk of the adjacent gas phase.

The first one is a convective heat transfer coefficient, and is estimated by dimensionless number correlations, as reported in *Appendix D*. The mass transfer coefficient is assumed equal to the heat transfer one by Lewis analogy[2]. No total pressure gradient and then no mass transfer resistance are assumed within the bed.

Extension of penetration theory to other contact drying applications

In 1987, another works by Tsotsas and Schlünder had extended the applications of vacuum contact drying to *hygroscopic material* (Tsotsas & Schlünder, 1987). In this work the presence of bound moisture X_h in the wet solid is not directly modeled, but its effects are taking into account with an additional term in the calculation of the effective specific heat capacity of the bed. If bound moisture is present, the heat capacity of the bed $c_{p,bed}$ is the sum of the specific heat capacity of the solid phase $c_{p,s}$ and the specific heat capacity of the residual bound moisture $c_{p,l}$. It is increased by the additional term as exposed below:

$$c_{p,bed} = c_{p,s} + X_h\, c_{p,l} - \Delta h_{ev} \left(\frac{\partial X_h}{\partial T}\right)_P \qquad (18)$$

[3] This model has been used in the thesis work and than more details about it can find later in the work.

This term is the product between the latent heat of vaporization Δh_{ev} and the local slope of the sorption isobar (solid-bound moisture vs. temperature)[4].

The influence of *poly dispersion* of particulate bed in the drying behaviour during vacuum contact drying was investigated by Tsotsas and Schlünder (Tsotsas & Schlünder, 1986). A modification of Schlünder and Mollekopf model for vacuum contact drying was developed in order to take into account the effect of particle segregation on drying rate curve.

Other examples of contact drying modelling extension using penetration theory are:

- solids wet by multi-component mixture (Martinez & Setterwalla, 1991)
- contact drying in presence of heated particulate medium (Tórrez & Martinez, 1994)

Also recent applications of penetration theory for industrial contact drying can be found elsewhere (Yan, et al., 2009).

Distribute parameter models for static bed

In the last decades, packed bed vacuum contact drying and intermittent stirring vacuum contact drying became very common in pharmaceutical industry, These techniques are used in order to avoid particle breakage and preserved the original particle shape (Kohout, Collier, & Stepanek, 2006). For that purpose a contact drying modelling of a packed bed with distribute parameter models was proposed by Kohout and co-workers (Kohout, Collier, & Stepanek, 2006). The model is based on the resolution of a set of differential mass and energy balances:

- liquid phase continuity equation;
- gas phase continuity equation;
- local energy equation;
- Darcy's law for the liquid phase;
- Darcy's law for the gas phase.

The set of time and space dependent partial differential equation is solved by a second-order finite difference discretization in space, and by explicit Euler method for time integration. A steady state model is also present in order to reduce the computational

[4] The slope of the sorption isobar is a negative value at every temperature. This justify the minus sign of the additional term.

time, but it should be applied only if the time scale of capillary mass flow is small enough than the evaporation rate time scale to allow a time scale separation. Several simulation results about the influence of some parameters are exposed in the work and also the comparison with some experimental results. This model give the local moisture and temperature distribution in *2D* or in *3D* inside the bed.

Recent lumped parameter models for static bed

In 2008, Michaud *et.al.* proposed two lumped parameter models for static bed contact drying simulation (Michaud, Peczalski, & Andrieu, 2008), inspired in Kohout *et.al.* model. In the first model called "*classical vaporization front mode*l" the Kohout *et.al.* approach is used for the simulation of constant rate period and falling rate period.

During the *constant rate period* is assumed that the vaporization occurs at the heating wall and the transport phenomena involved are:

- Heat transfer: conduction across the heating wall
- Mass transfer: vapour permeation across the bed (Darcy's law)

The simultaneous resolution of mass balance, energy balance and thermodynamic equilibrium (Antoine equation) give the moisture and temperature profiles.

During the *falling rate period* the drying front penetrated inside the bed. Now the transport phenomena that are taken into account in the model are:

- Heat transfer: - conduction across the heating wall
  - from the heating wall to first particle layer
  - across the bed (function of drying front position)

No more mass transfers are taken into account, because the heat conduction across the dry layer become more important than the vapour permeation across the wet part of the bed. The simultaneous resolution of mass balance, energy balance and thermodynamic equilibrium (Antoine equation) give the moisture and temperature profile and the drying front position.

Vacuum contact drying simulation with this model, in addition to physical property of solid phase and liquid phase and effective, required several parameters as: bed thermal conductivity, packed bed permeability of the vapour and critical solvent content. For

these parameters no prediction methods are suggested and the value used in the simulation are estimated as the best fitting on experimental drying rate curve.

The comparison between simulated and experimental drying curve show that this model is not able to precisely predict the drying rate in the falling rate period. For that reason some modifications are introduced, and the new model is called "Vaporization front model with a varying solvent supply".

The new topics are:

- a new drying phase, at the end of constant rate period, called "*transient period*". In this phase vaporization occurs in a thin zone near the heating wall, the transport phenomena are the same of the constant period with addition of the contact heat transfer;
- empirical correlation to calculate the moisture content at the drying front during falling rate period.

This modification introduced two new empirical parameters: Solvent supply parameter and the second critical solvent content.

4.2. Solid phase modelling

If the solid material particles are porous, the mass transfer inside the particle should be take into account in the modelling of the drying process. For highly heat sensitive materials like pharmaceuticals, biological material and foodstuff the temperature and the moisture content distribution within the wet solid being dried have a pronounced effect on the physiochemical states and on the local stress formation of the material (Chen, 2007). In order to calculate the temperature and moisture profile inside the wet solid during the drying process a distributed parameter model must be solved. In particular when the grain size is large the mass transfer should be controlled by internal diffusion and not by external mass transfer. The ratio between the external conductivity and internal conductivity is the *Biot number*. When $Bi>1$ the calculation of the drying rate by lumped parameter models should be an unacceptable approximation and the modelling of internal diffusivity should be taking into account (Mujumdar, 2007).

The solid phase temperature profile can be calculated from Fourier's equation:

$$\frac{\partial T}{\partial t} = \kappa_{eff} \frac{\partial^2 T}{\partial z^2} \tag{19}$$

And the moisture content profile can be calculated from *Fick's equation*:

$$\frac{\partial X}{\partial t} = \mathcal{D}_{eff} \frac{\partial^2 X}{\partial z^2} \tag{20}$$

where z is the direction normal to the particle surface and is assumed as the only one transport direction. Several set of boundary conditions for eq.(19) and eq.(20), and their resolution in different geometry can be found elsewhere (Carslaw & Jaeger, 1959) (Crank, 1975). Some details about the calculation of *Biot number* are also available (Mujumdar, 2007). Regarding contact drying calculation, a complete exposition of the resolution of the mass diffusivity problem applied to food and biological material was made by Chen (2007).

4.3. Modern modelling techniques

Discrete element method

Discrete element method (*DEM*) was developed by Cundall and Strack in 1979 (Cundall & Strack, 1979). This method give a discrete modelling of agitated particle bed by a description of individual particle motion based on mechanical principles. Introduction to DEM simulation applied to contact drying modelling can be found elsewhere (Metzger, Kwapinska, M., Saage, & Tsotsas, 2007), (Tsotsas, Kwapinska, & Saage, Modeling of contact dryiers, 2007). Purely mechanical DEM is by now well developed. Recent model upgrade includes thermal contacts between the particle, so that DEM models of heat transfer in contact dryers are now available, and then a full description of contact drying process may be possible. Commercial software for the mechanical and thermal DEM are available by ITASCA[5]. Discrete element method provides a realistically description of the mixing behaviour of a particle bed and then can overcome some limitation of penetration theory. The main limitation of this modelling technique is the computational resource.

[5] Name of the software: PFC

Pore network modelling

Pore network is a modelling technique able to describe drying of porous media at the pore level. The real porous medium is represented by a regularly or randomly located pores that are interconnected by throats. Different configuration of two or three dimensional pore network and different pore dimension are choosen in order to have the same structural property of the porous material. This kind of simulation is typically in the drainage problem, but in the past decade it become very important in the drying field. By the pore network simulation is possible to describe the pore solids drying behaviour in two way. First by estimation of the effective solid transport properties and second by direct simulation of the transport phenomena at pore level. The extension of the model to the mass transfer is an open research field, and is very important for a complete drying simulations. More detail about pore network modelling and the application to the drying process simulation is available in literature (Tsotsas, Kwapinska, & Saage, 2007).

Population balances

Population balances are applied to a particle bed, to describe the temporal change of the *number density distribution* of single particles with respect to different internal coordinate (velocity, dimension, etc.) and external coordinate (time and space). Applied to drying process simulation, the population balances provide the time an spatial evolution of particle properties, like temperature and moisture content. The application of population balance to drying are discussed in literature (Tsotsas, Kwapinska, & Saage, 2007).

4.4. Remarks

Stirred bed

The main problem in stirred bed contact drying is how to describe the effect of random particle motion on drying rate of particulate material. The first successfully approach was Penetration theory, a continuous bed model where the effect of the mixing are take in account by the empirical parameter call mixing number. A recent discrete approach called Discrete elements method, which take into account the bed mixing by resolution

of the moment equation for each particle. Despite the more detailed modelling of DEM, Penetration theory is choosen as starting point for the modelling and simulation in this Thesis work. The motivation are the follows (Tsotsas, Kwapinska, & Saage, Modeling of contact dryiers, 2007):

- Complete contact drying description by DEM have not reached maturity today;
- High computational cost of DEM simulation;
- Good performance of penetration theory demonstrated in several publications;
- Universality and versatility of penetration theory;
- Appropriate consideration of involved phenomena in penetration theory;
- Penetration theory is today the industrial standard to modelling the contact drying of agitated particle bed.

Packed bed

For packed bed simulations, three models were found in drying literature. The first one is based on Penetration theory, the penetration heat transfer coefficient is estimated form Mollekopf (1983) and the drying rate is computed following the vacuum contact drying modelling proposed by Schlünder and Mollekopf (1984). Good prediction of drying rate curves of non-hygroscopic materials are shown in the Schlünder and Mollekopf work of 1984. In this case, the only one empirical parameter of Penetration theory (mixing number) disappeared because the bed is static, then not parameter are required.

In the second model, by Kohout and co-workers (Kohout, Collier, & Stepanek, 2006), a dstribuite parameter approach is proposed, for the estimation of local moisture content and temperature inside the bed. However a greater computational cost is required comapred to the previous model.

The third model is basad on a lumped parameter approach (Michaud, Peczalski, & Andrieu, 2008), where the computational complexity is comparable to Penetration theory implementation. In this case, more transport phenomena are take into account, as the hygroscopic particle behaviour, but some experimental parameters are required for describe those.

Chapter 5

Models

5.1. General aspect

In this chapter the models used in the contact drying simulation are reported. The models regards two different applications:

- Vacuum contact drying of agitated particulate materials;
- Normal pressure contact drying of agitated particulate materials.

For each application a main contact drying model calculate the drying rate, the moisture content and the bed temperatures. The heat and mass transfer coefficients of the main model are estimated by appropriate models. For that estimation, models for effective properties of the bed, like bed thermal conductivity, are also required. At the last level the physical properties of gas and liquid phase are estimated. A qualitative scheme of the structure of the developed structure is reported in figure *5.1*.

The most suitable models choosen in the previous chapter are used for the main contact drying part and for the transport phenomena. The models used for effective properties are indicated in the text and the detail of the implementation are reported in appendixes. The physical an thermodynamic properties of gas and liquid phase are estimated as function of temperature and pressure following the models proposed in: "*Properties of gases and liquids*" (Reid, Prausnitz, & Poling, 1987). A database with the parameters of the models for 619 substances, from the same textbook, is used. Only the solid properties are set as input data. Now the models used in each one of the two applications are exposed in two different sections: *5.1*, and *5.2*, and inside each one, three sub-section regarding *contact drying model*, *heat/mass transfer models*, *effective properties models* are specified.

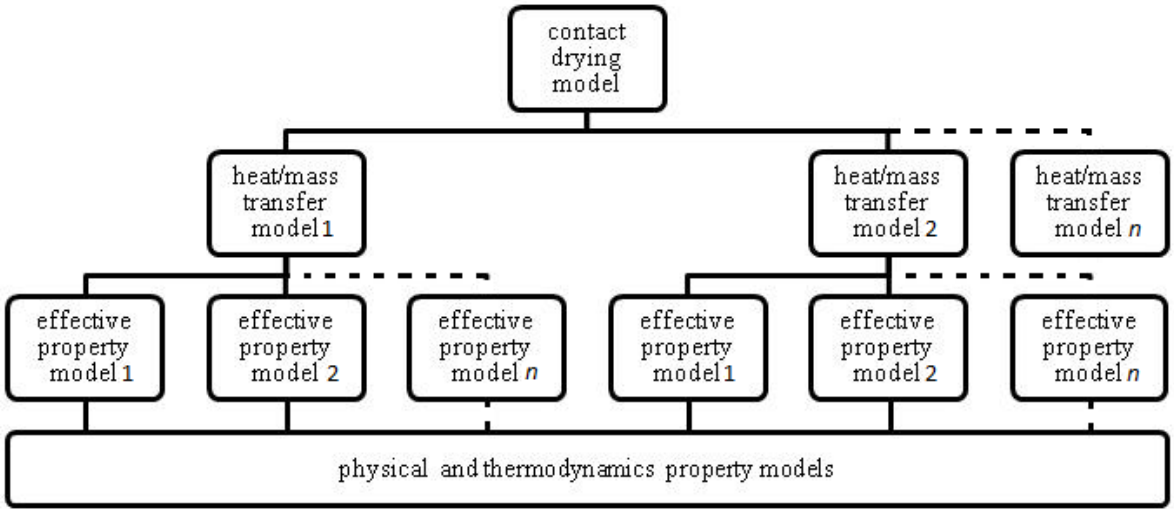

Figure 5.1. *Qualitative graphical representation of general "hierarchical structure" of the developed contact drying simulation models.*

5.2. Model for vacuum contact drying of stirred bed

A model for vacuum contact drying of agitated particulate material was build up. In this model the following assumption are made:

- The bed is assumed as a quasi-continuum with effective properties, and a moving drying front is assumed inside the bed following Penetration theory;
- Penetration theory is used in order to describe the effect of particle mixing on the drying rate. Perfect macro-mixing is assumed at the beginning of each contact period.
- The temperature at the heating surface is assumed to be known.

Then, the following transport phenomena are taken into account:

- Contact heat transfer;
- Heat penetration transfer.

Internal mass and heat transport are ignored in the general case and then are not modelled. Vapour mass transfer across the particle bed is also neglect. Other mass transport phenomena are not taken into account because of the vacuum.

Now the general model for vacuum contact drying and all the models used for the estimation of the required heat transfer coefficient and effective properties are exposed.

Contact drying model

The main contact drying model is based on the Schlünder and Mollekopf (1984). The principle of the model and the equations are reported below.

In vacuum contact drying, the saturation temperature of the moisture $T_s(P)$ is lower than the normal saturation temperature, and usually is also lower than the normal room temperature. When the wet particle material at room temperature or higher is put in contact with a hot surface at temperature T_w the vaporization started and all the bed reach the saturation condition: $T_b = T_s(P)$ by loss of latent heat of vaporization. In the first instant the whole bed is at saturation condition then no heat penetration resistance in the bed occur. The only one resistance is the heat contact resistance, and the heat flux shows a maximum value. This value is the *maximum drying rate for vacuum contact drying* and it can be calculated by:

$$\dot{m}_{max} = \frac{\dot{q}_0}{\Delta h_v} = \frac{\alpha_{ws}\big(T_w - T_s(P)\big)}{\Delta h_v} \tag{21}$$

But immediately after, the moisture content of the bed starts to fall down then the presence of dry particle in the bed produce a resistance in the heat penetration inside it. The overall heat transfer coefficient that take into account both contact resistance and penetration resistance for wet and dry bed can be estimated by penetration theory as exposed above.

Now, the heat flux can be calculated with a lumped parameter model as a function of the temperature gradient between the heating wall and the bulk of the bed:

$$\dot{q}_0 = \alpha_{wet}(T_w - T_b) \tag{22}$$

This flux corresponding with the continuously heat flux *at the wall surface*. The relative heat flux *at the drying front position* can be calculated from the previous heat flux:

$$\dot{q}_{z_T} = \dot{q}_0 \exp(-\zeta^2) \tag{23}$$

where the reduced position of drying front ζ can be evaluated by Penetration theory as shown in *Appendix B*. This second one heat flux is less than the first one, because part of the heat flux is spend to rise up the temperature of the already dry particle between the hot surface to the drying front. At the beginning of the drying process, all the particle are still wet, there is not dry particle, and then all the heat flux from the hot surface $\dot{q}_0$ is used to evaporated the moisture. But, as the drying process going on, there

are some dry particles in the bed, and part of heat is spend to increase its temperature $\dot{q}_{sen}$. The remaining heat flux available for the moisture evaporation is $\dot{q}_{z_T} = \dot{q}_0 - \dot{q}_{sen}$ and then the drying rate is calculated as:

$$\dot{m} = \frac{\dot{q}_{z_T}}{\Delta h_{ev}} = \frac{\dot{q}_0 \exp(-\zeta^2)}{\Delta h_{ev}} \tag{24}$$

In this way, the effect of the increase of probability of dry particle heating, as the drying process is going on, is takes into account. In this situation, a bed temperature raising occur as the drying process going on. The temperature rise during each contact period, and it is give by a energy balance. The equation used is:

$$\Delta T_b = \frac{\Delta h_{ev}}{c_{p,l}} \frac{1 - \exp(-\zeta^2)}{\exp(-\zeta^2)} \Delta X \tag{25}$$

Calculation of heat transfer coefficients

Contact heat transfer coefficient

The model used is the Schlünder one exposed in the previous chapter. The model and all the eqaurtions for the implementation are reported in *Appendix A*. The contact heat transfer coefficient is calculated as a function of particle diameter, gas phase thermal conductivity, gas phase specific heat capacity and gas phase molecular weight. In a vacuum operation the gas phase properies are referred to the vapour moisture. Some coefficients are also used in the model and the values are taken form Schlünder and Mollekopf 1984 and reported them at table *5.1*.

Table 5.1. *Parameters used for the contact heat transfer coefficient estimation.*

Plate surface coverage factor	ϕ_A	0,80	-
Accommodation coefficient	γ	0,80	-
Black body radiation coefficient	σ	5,67 10^{-8}	W/m^2,K^4
Stefan-Boltzmann const. for radiation	C_{12}	0.85 σ	W/m^2,K^4

Heat penetration coefficient

Penetration theory is used for the heat penetration coefficient estimation. Eq. (11) presented in the previous chapter is used, and the contact time is estimated by using eq.(12) and (14)[6]. The reduced position of the drying front ζ, can be calculated by iterative solution on the following equation:

$$\sqrt{\pi}\,\zeta \exp\zeta^2 \left[\left(\frac{\alpha_{ws}}{\alpha_{dry}} - 1\right)\operatorname{erf}\zeta + 1\right] = \frac{1}{Ph}\left(\frac{\alpha_{ws}}{\alpha_{dry}} - 1\right) \tag{26}$$

where α_{dry} is the overall heat transfer coefficient of a totally dry bed:

$$\frac{1}{\alpha_{dry}} = \frac{1}{\alpha_{ws}} + \frac{1}{\alpha_{sb,dry}} \tag{27}$$

The heat penetration coefficient of dry bed $\alpha_{sb,dry}$ can be calculated by eq. (6) proposed by Wunschmann and Schlünder for dry agitated beds. In eq. (26) Ph is the *phase-change number* (also called as *reduced average moisture content of the bulk*) and is a measure of the intensity of the latent heat sink. It is defined as, and it can be calculated from:

$$Ph = \frac{X\,\Delta h_{ev}}{c_{p,dry\,bed}(T_w - T_s)} \tag{28}$$

Estimation of effective properties

Penetration theory assumed effective proprieties of the bed. If the theory is applied to the vacuum contact drying, the effective proprieties are referred to the dry bed. That is because the heat penetration occurs from the heating wall to the drying front, and in this zone of the particle bed is assumed totally dry at the end of each contact period.

Dry bed specific heat capacity

The dry bed specific heat capacity is assumed equal to the specific heat capacity of the particulate solid.

[6] In eq.(14) parameter from (Schlünder & Mollekopf, 1984) are used.

Bulk density of the bed

The bulk density of the bed is calculated from the density of the non porous solid by the following equation:

$$\rho_{dry,bed} = \rho_s(1-\varepsilon_b)(1-\varepsilon_p) \quad (29)$$

Dry bed thermal conductivity

In order to estimate the effective dry bed thermal conductivity $\lambda_{dry,bed}$ one of the most common theory is the *"Parallel cell heat flux model"* developed by Zehner (1973) and Bauer (1982), summarized in English by Schlünder (1984). A detailed description of the model can be found in the Tsotsas and Martin's review (1987). In that review the Zehner and Bauer theory is indicated as: "the recommended one for engineering use for its good agreement with experimental data".

In this approach the thermal conductivity of dry bed is a function of the thermal conductivity of the solid, the thermal conductivity of the gaps between the particles, and two equivalent thermal conductivity due to radiation and to molecular flow. The model can be applied to mono-dispersed as well as poly-dispersed packed beds of spherical and non spherical particles of poor and good conductors within a wide temperature and pressure range ($100 < T < 1'500$ K; $1 \cdot 10^{-3} < P < 100$ bar) (Schlünder & Mollekopf, 1984). The parameters of the model that were used in the simulations are reported in table *5.2*.

The equations for the estimation of the bed thermal conductivity of a mono-disperse particulate bed are used in this work, and reported in *Appendix C*.

Table 5.2. *Parameters of Zehner and Bauer model for effective thermal conductivity of particulate beds. Values for ceramic powders. (Schlünder & Mollekopf, 1984)*

Shape factors for interstitial energy transport:	by radiation	R_{form}	1
	by convection	C_{form}	1
	Relative flattened particle – surface contact area	ϕ_k	0.0077

5.3. Model for normal pressure contact drying of stirred bed

In the model for normal pressure contact drying the following assumption are made:

- The bed is assumed as a continuum with effective properties;
- Penetration theory is used in order to describe the effect of particle mixing on the drying rate. Perfect macro mixing is assumed at the beginning of each contact period.
- Unit value of Lewis number about the heat and mass transfer from the free surface of the bed to the bulk of the gas phase;
- No total pressure gradient exist within the bed, then no mass transfer resistance is assumed across the bed.
- The temperature at the heating surface is assumed to be known.

Then, the following transport phenomena are taken into account:

- Contact heat transfer;
- Heat penetration transfer;
- Heat transfer to the gas phase above the bed;
- Mass transfer to the gas phase above the bed.

Internal mass and heat transport are ignored in the general case, and then are not modelled. Also mass transport phenomena across the particle bed are not take in account. Now, the general model for vacuum contact drying and all the models used for the estimation of the required heat transfer coefficient and effective properties are presented.

Contact drying model

The contact drying model for normal pressure simulations is based on the work of Tsotsas and Schlünder (1986). The modelling of this process will be discussed in this section.

The main difference between the vacuum and normal pressure contact drying, in the calculation of the drying rate, is that: in the vacuum case first the heat transfer problem is resolved and the latent heat flux is calculated and then the drying rate is calculated

from it; in normal pressure case, first the drying rate is estimated from the gas phase mass transfer equation, and then the latent heat and the other heat flux are obtained. The estimation of the drying rate and how to obtain the different heat fluxes are discussed below.

Mass transfer equation

In presence of a gas phase, drying usually occur by vaporization below the saturation temperature of the moisture at the operating condition, by mass transfer from the wet solid to the gas phase. The lumped parameter equation for the interphase mass transfer of moisture from the bed surface to the inert gas phase with a logarithmic drying force is:

$$\dot{n} = \frac{\rho_g}{MW_g}\ \beta\ ln\left(\frac{P - p_g}{P - P_s(T_o)}\right) \tag{30}$$

The molar drying rate $\dot{n}$ is calculated by the logarithmic drying force between the moisture partial pressure in gas phase p_g and the moisture partial pressure in liquid phase, that is equal in case of unbound moisture to the saturation pressure at the operating temperature. The gas phase mass transfer coefficient β can be estimated from the convective heat transfer coefficient in the gas phase, by assuming a unit value of *Lewis number* (Lewis analogy):

$$Le = \frac{heat\ transfer\ conductivity}{mass\ transfer\ conductivity} = \frac{MW_l\ \alpha_c}{c_p\ \rho_g\ \beta} = 1 \tag{31}$$

Then the expression for the mass drying rate becomes:

$$\dot{m} = \frac{MW_l}{MW_g}\ \frac{\alpha_c}{c_p}\ ln\left(\frac{P - p_g}{P - P_s(T_0)}\right) \tag{32}$$

where α_c can be estimated as shown in *Appendix D*.

Energy balances

In contact drying in presence of gas phase there are five heat fluxes, show in figure *5.2* with the relative profile temperature. The heat flow from the heating wall to the particle bed is now called $\dot{q}_{in}$ instead $\dot{q}_0$ and it can be calculated from:

$$\dot{q}_{in} = \alpha_{ws}(T_w - T_H) = \alpha_{sb}(T_H - T_b) \tag{33}$$

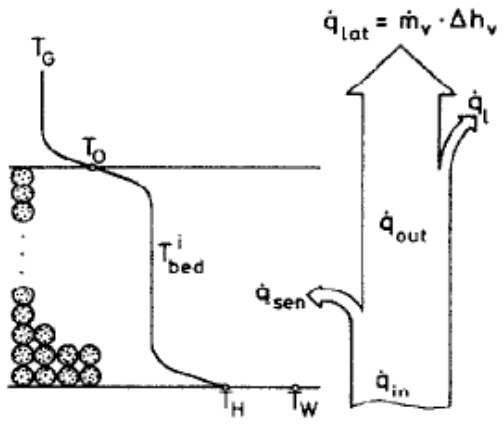

Figure 5.2. *Qualitative representation of temperature profiles and het fluxes in contact drying at normal pressure. (Tsotsas & Schlünder, 1986)*

This heat flux is split in two part. One is the sensible heat flux $\dot{q}_{sen}$ that produces a bed temperature increase:

$$\dot{q}_{sen} = \left(\rho\, c_p\right)_{bed,wet} h\ \frac{\Delta T_b}{t_i} \tag{34}$$

where h is the height of the bed and ΔT_b is the bed temperature variation during the time t_i[7]. The other one is the flux that leave the bed to the surface in contact with the gas phase $\dot{q}_{out}$:

$$\dot{q}_{out} = \alpha_{sb,wet}(T_b - T_o) \tag{35}$$

The heat flux $\dot{q}_{out}$ is the sum of the latent heat of vaporization flux $\dot{q}_{lat}$ that can be calculated from the drying rate from:

$$\dot{q}_{lat} = \dot{m}\ \Delta h_v \tag{36}$$

and the heat flux loss by increasing the gas phase temperature $\dot{q}_{lat}$ that and can be calculated by:

$$\dot{q}_l = (\alpha_c + \alpha_r)\left(T_o - T_g\right) \tag{37}$$

The main relations that relate the several heat fluxes are then:

$$\dot{q}_{in} = \dot{q}_{sen} + \dot{q}_{out} \tag{38}$$

$$\dot{q}_{out} = \dot{q}_{lat} + \dot{q}_l \tag{39}$$

[7] t_i is the time step of the iteration cycle in the simulation. The choice of that value is a numerical question and is described in the next chapter.

Model equations

Evaluation of drying rate and the surface temperature T_0 can be carried out by simultaneous iterative solution of the following equation:

$$\begin{cases} \dot{q}_{out} - \dot{q}_l = \dot{m}\ \Delta h_v \\ \dot{m} = \dfrac{MW_{liq}}{MW_{gas}}\ \dfrac{\alpha_c}{c_p}\left(\dfrac{P - p_g}{P - p_s(T_o)}\right) \end{cases} \tag{40}$$

The first equation compare the latent heat flux from eq.(39) to the same heat flux from eq.(2), and the second one equation is eq.(32). If the lumped parameter model for the two heat flux is substituted into the first equation the system becomes:

$$\begin{cases} \left[\alpha_{sb,wet}(T_b - T_o)\right] - \left[(\alpha_c + \alpha_r)\ (T_o - T_g)\right] = \dot{m}\,\Delta h_v \\ \dot{m} = \dfrac{MW_{liq}}{MW_{gas}}\ \dfrac{\alpha_c}{c_p}\left(\dfrac{P - p_g}{P - p_s(T_o)}\right) \end{cases} \tag{41}$$

If the saturation pressure is expressed as a function of T_o by Antoine equation, the system have only 2 unknown variables $\dot{m}$ and T_o and the solution can be reached. Now $\dot{q}_{out}$, $\dot{q}_l$, $\dot{q}_{lat}$ can be backward calculated.

The values of T_H and $\dot{q}_{in}$ are obtained by simultaneous resolution of the two expressions for $\dot{q}_{in}$ in eq.(34):

$$\begin{cases} \dot{q}_{in} = \alpha_{ws}(T_w - T_H) \\ \dot{q}_{in} = \alpha_{sb}(T_H - T_b) \end{cases} \tag{42}$$

and by one the possible explicit of the unknown value yields:

$$\begin{cases} T_H = \dfrac{\alpha_{ws}T_w + \alpha_{sb}T_b}{\alpha_{ws} + \alpha_{sb}} \\ \dot{q}_{in} = \alpha_{sb}(T_H - T_b) \end{cases} \tag{43}$$

Now the sensible heat flux can be calculated by inverse of eq.(37):

$$\dot{q}_{sen} = \dot{q}_{in} - \dot{q}_{out} \tag{44}$$

And then, the drying rate and all the heat fluxes in the dryer are calculated.

Calculation of heat transfer coefficients

Contact heat transfer coefficient

Also in this case the model used for contact heat transfer coefficient is the Schlünder model explained in the previous chapter. In *Appendix A* there is the detail for the model implementation and all the equations.

Heat penetration coefficient

Application of penetration theory to normal pressure contact drying proposed by Tsotsas and Schlünder, and described in the previous chapter, was used. Then, the heat transfer coefficient is calculated by Eq. (17), and the contact time is estimated by using eq.(12) and (14)[8]. In this case no any solution for the position of the drying front is required, then, the equation can be directly applied.

Convective and radiative heat transfer coefficient

Convective heat transfer coefficient at the free surface of the bed is estimated by dimensionless number relations using *Nusselt number*. Radiative heat transfer coefficient is calculated from Stefan-Boltzmann law. Detail about the calculation of both the heat transfer coefficients are shown in *Appendix E*.

Estimation of effective properties

When the penetration theory is applied to the contact drying in presence of normal pressure, the analytical solution of the temperature profile between the heating wall and the free surface are referred to partially wet bed.

Wet bed specific heat capacity

The wet bed specific heat capacity $c_{p,wet}$ is calculated by taking into account both the solid $c_{p,s}$ and moisture $c_{p,l}$ specific heat capacity:

$$c_{p,wet} = c_{p,s}\, x_s + c_{p,l}\, x_l \tag{45}$$

where x is the mass fraction of each phase in the bed.

[8] In eq.(14) parameter from (Schlünder & Mollekopf, 1984) are used.

Eq. (45) can be written more compactly as:

$$c_{p,wet} = c_{p,s} + X\, c_{p,l} \tag{46}$$

Bulk density of the wet bed

The bulk density of the wet bed is calculated from the density of the non porous solid and the density of the liquid by the following equation:

$$\rho_{dry,bed} = v_s\, \rho_s (1 - \varepsilon_b)\left(1 - \varepsilon_p\right) + \; v_l\, \rho_l \tag{47}$$

where v is the volume fractions of each phase.

Wet bed thermal conductivity

The wet bed thermal conductivity $\lambda_{wet,bed}$ is estimated according to the Zehner and Bauer model that is used also in vacuum contact drying modelling, and explained in *Appendix C*. As seen before, in this approach the thermal conductivity of the bed is function of the thermal conductivity of the solid, the thermal conductivity of the gaps between the particle, and two equivalent thermal conductivity due to radiation and to molecular flow. For a wet bed, the thermal conductivity of the solid and the thermal conductivity of the gaps between the particle must to be estimated respectively for a wet solid and for a wet gas phase in the gaps.

In order to take into account the presence of the liquid phase in the estimation of these two thermal conductivities the model developed by Krischer is used (Krischer, 1963). Some description in English of Krischer model can be found elsewhere (Tsotsas & Schlünder, 1986). In this model a series/parallel combination of thermal conductivities of the solid phase, of the liquid, of the gas in the interparticle gaps and in the particle pore are taken into account. Heat transfer due to evaporation of the liquid phase, vapour diffusion and recondensation in the interparticle gaps and in the particle pore are also taken into account by an effective thermal conductivity term. All the equations of the model are reported in *Appendix D*.

Chapter 6

Simulation programs

6.1. General aspects

For contact drying of particulate material, simulation programs were developed, based on the model exposed in the previous section. The aim of the simulation programs are the calculation of:

- time profile of moisture content;
- time profile of drying rate;
- time profile of mean bed temperature.

From the first two results drying rate curve can be computed. In these programs all the physical and thermodynamic properties of gas and liquid phase, and all the effective properties are evaluated by appropriate model as function of pressure and actual temperature and moisture content of the bed.

The programs are based on a main iteration cycle, starting with initial moisture content and temperature of the bed. At each cycle the main program give the instantaneous moisture and temperature bed variation, and the instantaneous drying rate. The moisture and temperature variation are used to calculate the new bed temperature for the next cycle. Every cycle represent a time step and its length is the maximum one for a stable and accurate solution. At every cycle the value of all the physical properties of gas and liquid phases are updated at the new temperature; and the effective properties are updated at the new value of physical properties, temperature and moisture content. The calculation cycle continue until the bed are totally dry ($X \cong 0$) or the time reach the "end time" of the simulation fixed as an input data.

Therefore, the simulation algorithm can resumed as follow:

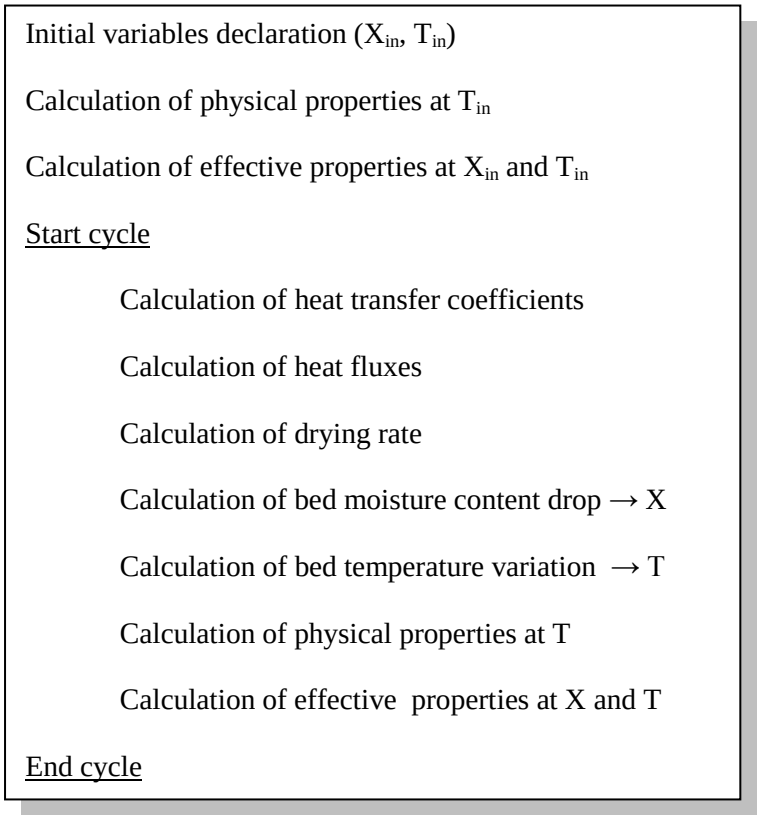

Figure 6.1. G*eneral structure of the contact drying simulation programs.*

All the calculation are made in several programs. There is a *main* program where the mass and energy balance in the dryer are solved, and drying rate and bed temperatures are calculated. The required heat/mass transfer coefficients and the effective properties are estimated in several sub-programs. At the end, a set of programs for physical and thermodynamic properties evaluation give the value of the required properties. A graphical representation of the iteration cycle, and the connection between the program, are reported in figure *6.2*.

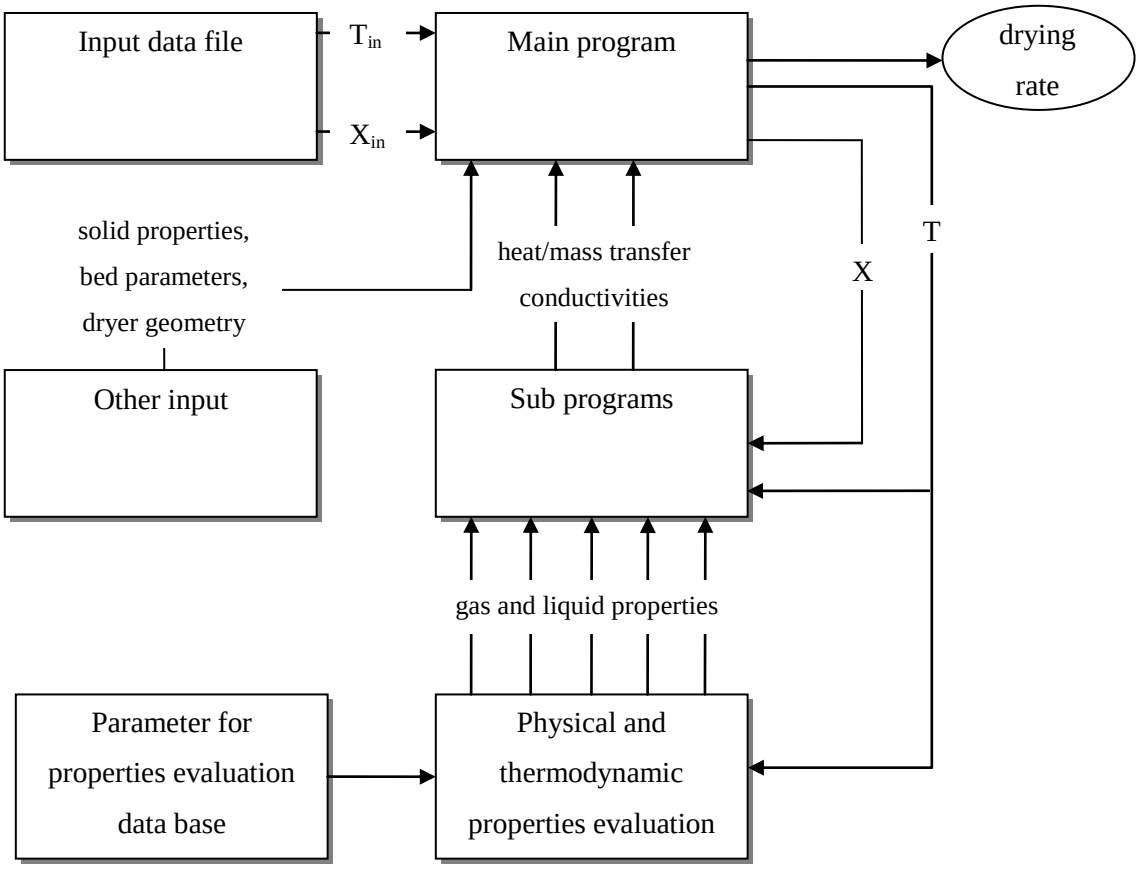

Figure 6.2. *Graphical representation of the iteration structure in contact drying programs.*

Some detail about the simulation of each contact drying process are reported in the following sections.

6.2. Vacuum contact drying program

In Figure *6.3* a detailed graphical scheme of the developed vacuum contact drying of agitated beds program is presented. A scheme of the program's algorithm is exposed in *Appendix E*.

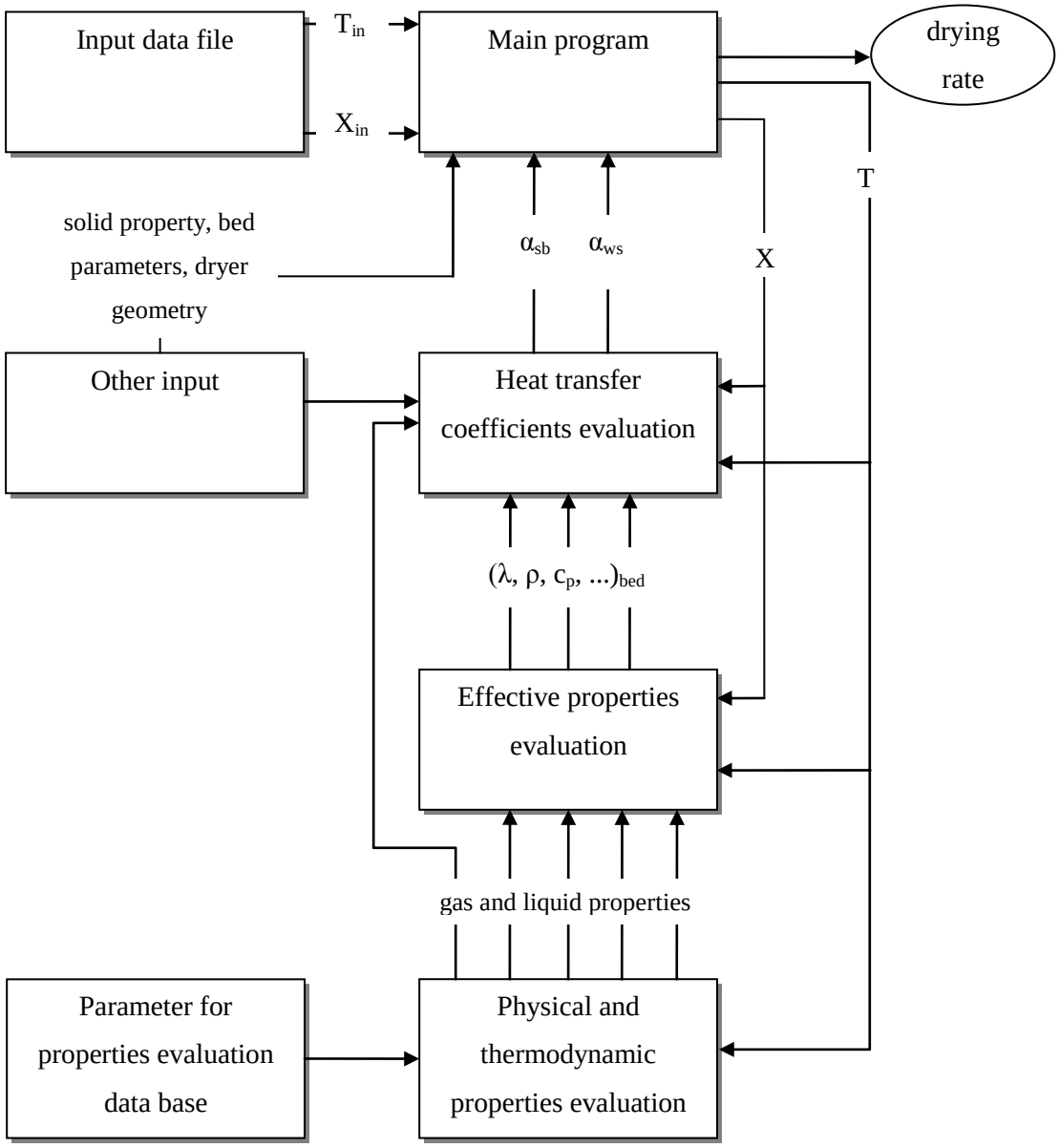

Figure 6.3. *Graphical representation of the detailed structure in the developed vacuum contact drying of agitated beds program.*

In the scheme of figure *6.3* four programs level can be found:

- *1° Level:* main program
- *2° Level:* programs for heat transfer calculation
- *3° Level:* programs for effective properties evaluation
- *4° Level:* programs for physical and thermodynamic properties evaluation

At the *first level* the main program make the resolution of energy balances in order to calculate drying rate, moisture content drop and temperature variation of the bed.

The input data for the first step are:

$$X = X_{in} \tag{48}$$

$$T_b = T_{sat}(P) \tag{49}$$

At each step, the relative position of the drying front ζ is calculated by iterative solution of eq. (25), and then the heat penetration coefficient is computed. After that, the heat flux at the surface, the drying rate and the bed temperature rise can be calculated. The moisture content drop ΔX can be assigned as a constant value, otherwise can be calculated from the amount of moisture evaporated during the current contact period:

$$\Delta X = \frac{\dot{m}\, A\, t_R}{M_{dry}} \tag{50}$$

In this work, the second choice was adopted.

At the *second level* three programs are required in order to calculate three heat transfer coefficients:

- *radiative heat transfer coefficient* (function of temperature);
- *contact heat transfer coefficient* (function of: temperature, pressure, radiative heat transfer coefficient, particle diameter, roughness, gas thermal conductivity, gas specific heat capacity);
- *heat penetration coefficient* (function of: bed density, bed thermal conductivity, bed specific heat capacity, contact time).

where:

- *contact time* is function of: stirring frequency, mixing number, position of drying front;
- *mixing number* is function of: Froude number, two empirical coefficients;
- *position of drying front* is function of: enthalpy of vaporization, moisture content, solid specific heat capacity, temperature, contact heat transfer coefficient.

In the *third level* all the effective properties are estimated. The list is:

- *bed specific heat capacity* (function of solid specific heat capacity);
- *bed density* (function of solid density, solid porosity, bed porosity);

- *bed thermal conductivity* (function of solid thermal conductivity, liquid thermal conductivity, gas thermal conductivity, gas specific heat capacity, temperature, pressure, particle diameter, shape factors).

At the *fourth level*, six physical and thermodynamic properties are estimated as function of actual bed temperature:

- liquid density (function of temperature);
- liquid latent heat of vaporization (function of temperature);
- gas specific heat capacity (function of temperature);
- liquid specific heat capacity (function of temperature);
- liquid thermal conductivity (function of temperature);
- gas thermal conductivity (function of temperature).

Then, starting from the initial values of:

- initial bed temperature,
- initial moisture content of the bed,

a set following of operating variables:

- pressure,
- heating wall temperature,
- stirring frequency,
- mass of solid,

the bed geometry:

- bed diameter,
- bed porosity,

the name of the component of the gas phase and liquid phase for properties evaluation, the following set of fixed solid phase properties:

- solid density (intrinsic density),
- solid porosity,
- particle roughness,
- solid thermal conductivity,
- solid specific heat capacity,
- particle shape factors,

and the empirical coefficients for mixing number, drying rate curve can be computed. Excepted solid phase properties, all the property required for the simulation are estimated in the program. The value of the solid phase properties, could be known, as well as the parameter for mixing number estimation, otherwise they should be found in literature. Excluding that, the calculation of drying rate and bed temperatures with this program is *predictive,* i.e. the drying rate can be computed only with initial values, operating variables and bed geometry as input data.

6.3. Normal pressure contact drying program

The calculation algorithm structure is slightly different from the vacuum contact drying case. A detailed scheme of normal pressure contact drying simulation program is exposed in Figure *6.4* and a scheme of the algorithm procedure is exposed in *Appendix F*.

From Figure *6.4* the simulation program is based in five program level:

- *1° level:* main program;
- *2° level:* iterative resolution of heat and mass balances;
- *3° level:* programs for heat transfer calculation;
- *4° level:* programs for effective properties evaluation;
- *5° level:* programs for physical and thermodynamic properties evaluation.

At the *first level*, in the main program there is the calculation of moisture content drop and temperature variation of the bed. The input data for the first cycle are:

$$X = X_{in} \tag{51}$$

$$T_b = T_{in} \tag{52}$$

The bed temperature rise can be computed from the sensible heat flux by inversion of eq.(35):

$$\Delta T_b = \frac{\dot{q}_{sen}\, t_R}{h\,(\rho\, c_p)_{bed,wet}} \tag{53}$$

At the end the moisture content drop can be calculated with eq.(50) as in vacuum contact drying case.

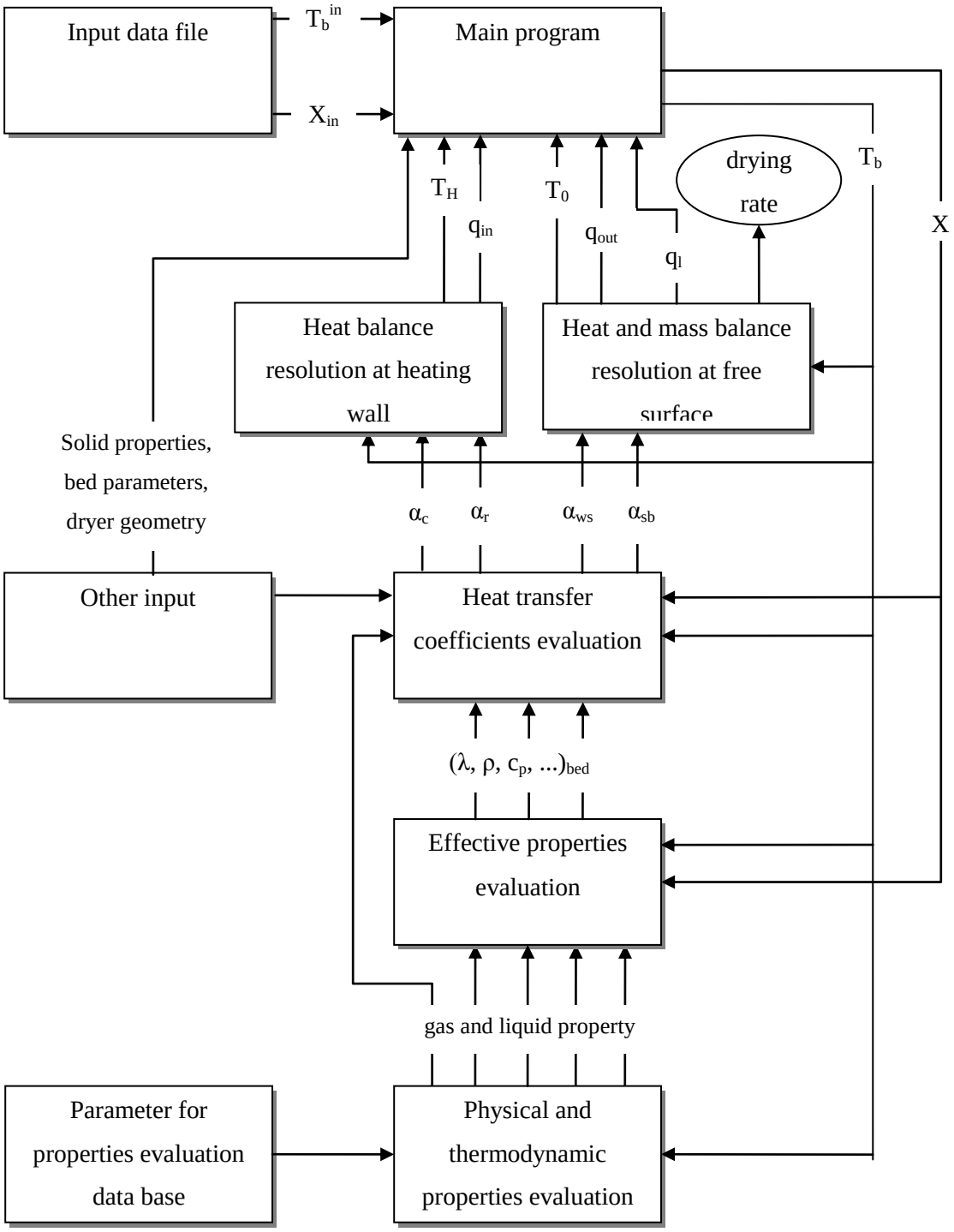

Figure 6.4. *Graphical representation of the detailed structure of the developed normal pressure contact drying of agitated beds program.*

At *second level*, there are two iterative programs for mass and energy balances resolution. In the first one (the one on the right in Figure *6.4*), the mass and energy balances at the free surface of the bed are simultaneously resolved in order to calculate

free surface temperature, drying rate, and heat fluxes. In the latter, energy equation at the heating wall is resolved in order to calculate the first particle layer temperature and the heat flux. In both the programs an unknown value is the temperature, but for the physical and thermodynamic properties estimation, effective properties and the value of heat transfer coefficient that are function of temperature, a known value of temperature is required. For this reason, an iteration cycle on the unknown temperature value is required. In the first program cycle can be integrated in the existing one, in the second program an iteration cycle is applied [9].

At the *third level* there are four program, for estimation of each heat transfer coefficients [10]:

- *radiative heat transfer coefficient* (function of temperature);
- *contact heat transfer coefficient* (function of: temperature, pressure, radiative heat transfer coefficient, particle diameter, roughness, gas thermal conductivity, gas specific heat capacity);
- *heat penetration coefficient* (function of: bed density, bed thermal conductivity, bed specific heat capacity, contact time);
- *convective heat transfer coefficient* (function of: pressure, bed temperature, gas temperature, gas moisture content, gas velocity, gas thermal conductivity, gas specific heat capacity, gas viscosity, bed diameter);

where:

- *contact time* is function of: stirring frequency, mixing number, position of drying front;
- *mixing number* is function of: Froude number, two empirical coefficients.

In the *fourth level* all the effective properties are estimated. The list is:

- *bed specific heat capacity* (function of: solid specific heat capacity, liquid specific heat capacity, moisture content);

[9] This temperature cycle that involve a recalculation at every iteration of all the value that are function of temperature is not indicated in figure *6.3* for simplicity but is used in the programs.

[10] Remember that the calculation of convective mass transfer coefficient is not required by using the Lewis analogy.

- *bed density* (function of: solid density, solid porosity, bed porosity, liquid density, moisture content);
- *bed thermal conductivity* (function of: solid thermal conductivity, liquid thermal conductivity, gas thermal conductivity, solid moisture content, gas moisture content, solid density, liquid density, solid porosity, gas specific heat capacity, temperature, pressure, particle diameter, shape factors).

At the *fifth level* seven physical and thermodynamic properties are estimated as function of pressure and actual bed temperature:

- liquid density (function of temperature);
- gas density (function of temperature and pressure);
- liquid latent heat of vaporization (function of temperature);
- gas specific heat capacity (function of temperature);
- liquid specific heat capacity (function of temperature);
- liquid thermal conductivity (function of temperature);
- gas thermal conductivity (function of temperature).

Then, starting from the initial values:

- initial bed temperature,
- initial moisture content of the bed,

a set following of operating variables:

- pressure,
- heating wall temperature,
- stirring frequency,
- mass of solid,
- gas velocity,
- gas moisture content,

the bed geometry:

- bed diameter,
- bed height,
- bed porosity,

the name of the component of the gas phase and liquid phase for properties evaluation,

the following set of fixed solid phase properties:

- solid density (intrinsic density),
- solid porosity,
- particle roughness,
- solid thermal conductivity,
- solid specific heat capacity,
- particle shape factors,

and the empirical coefficients for mixing number, drying rate curve can be computed. Also in this case, excepted solid phase properties, all the properties required for the simulation are estimated in the program. The value of the solid phase properties could be known, as well as the parameter for mixing number estimation, otherwise they should be found in literature. Excluding that, the calculation of drying by this program rate is *predictive* i.e. the drying rate can be computed only with initial values, operating variables and bed geometry as input data. In this case two more operating variable compare respect to vacuum case, relatively to the gas phase (gas velocity and gas moisture content), and one more geometrical property of the bed (high of the bed).

Chapter 7

Results

In the previous chapter, two programs for two different contact drying processes were presented. In this chapter, the results of these programs are presented and described in details. The results for each contact drying operation are reported separately in the paragraphs *7.1* and *7.2*. In each one paragraph, first there is a description of the simulation results, later a comparison between the simulation results and experimental data, at different operating condition, and an analysis of the influence of the operation condition in the results are reported.

All the simulation results concern contact drying in a *particulate bed disc dryer*. Two common pharmaceutical excipients: *talc* and *kaolin* are dried. Talc (or *talcum*) is a crystalline powder of *hydrated magnesium silicate*. It is one of the most common lubricant for tablets, capsules and powders and one of the most used diluents for pharmaceutical powders. Kaolin (or *kaolinite*) is a crystalline powder of *hydrated aluminium silicate*. It is an excipient for tablets and is also used as a active ingredient: internally for stomach pain and typically as an emollient agent. These two compounds are selected because they are found in a wide range of pharmaceuticals, sometimes in large amounts, then the mean drying behaviour of pharmaceutical compound can be approximately represent by the drying behaviour of these compounds. In addition, experimental data for these excipients are available in literature. The liquid phase that is removed during the process is *water*, one of the most common solvent in the pharmaceutical process.

7.1. Vacuum contact drying

Simulation results

The results of the simulation program are presented here. The profile of all the calculated properties that are varying during the drying process are presented. All the results exposed in this section are referred to the input data of simulation *A.1* reported in *Appendix F*.

Drying rate and temperature profile

The simulation results, with the main importance in the industrial application, are the drying rate profile and the temperature profile of the bed. These results are shown in figure *7.1*.

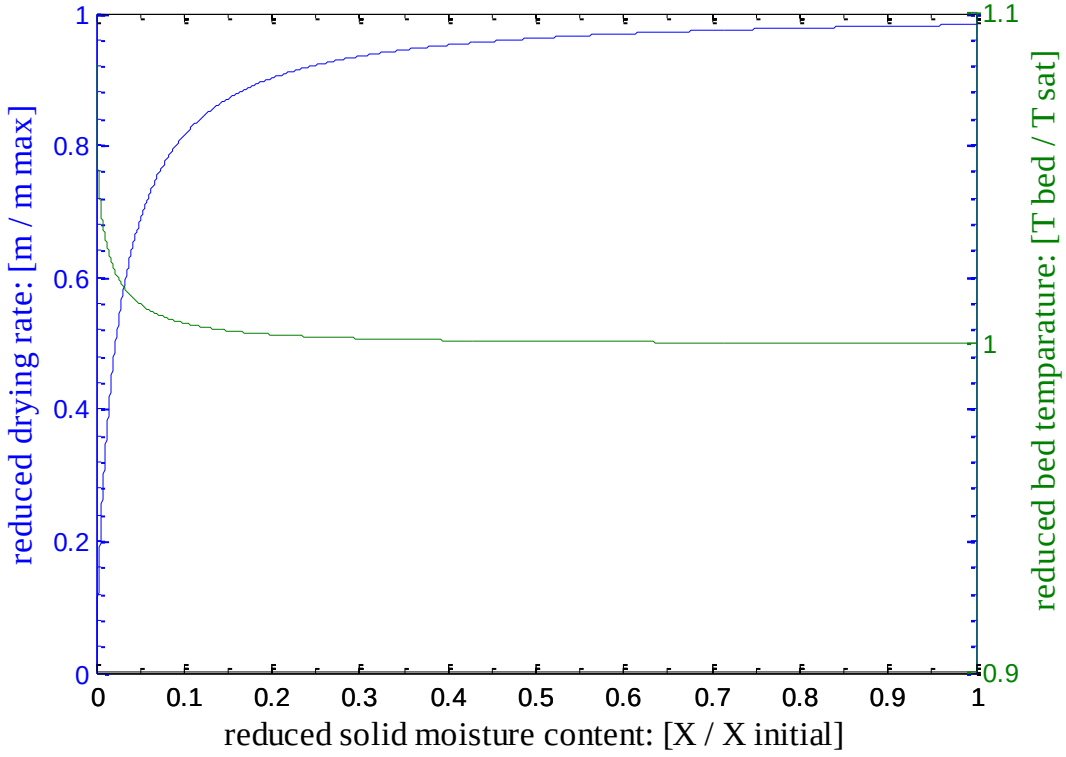

Figure 7.1. *Normalized drying rate curve and normalized bed temperature during vacuum contact drying of agitated particulate material, as a function of reduced moisture content. Input data set: Sim. A.1*

The *drying rate* starts from a high value, close to the maximum drying rate. Then the profile follows the overall heat coefficient profile (reported later), with a slightly

decreasing stage, and a fall down at the end, due to the depth penetration of the drying front. For a totally dry bed the model predict correctly a zero value of the drying rate.

The *bed temperature* starts very close to the saturation temperature at the operation pressure, and is almost constant for a long part of the process, because the evaporation takes place at the saturation temperature. Only when a great part of the particles are already dry, the "overheating" effect[11] produce an evident temperature increase. Anyway the global temperature rise of the bed is not large.

Heat transfer coefficients profiles during contact drying

Regarding thermal coefficients profiles during vacuum contact drying of agitated particulate materials, the simulation results are shown in figure *7.2*.

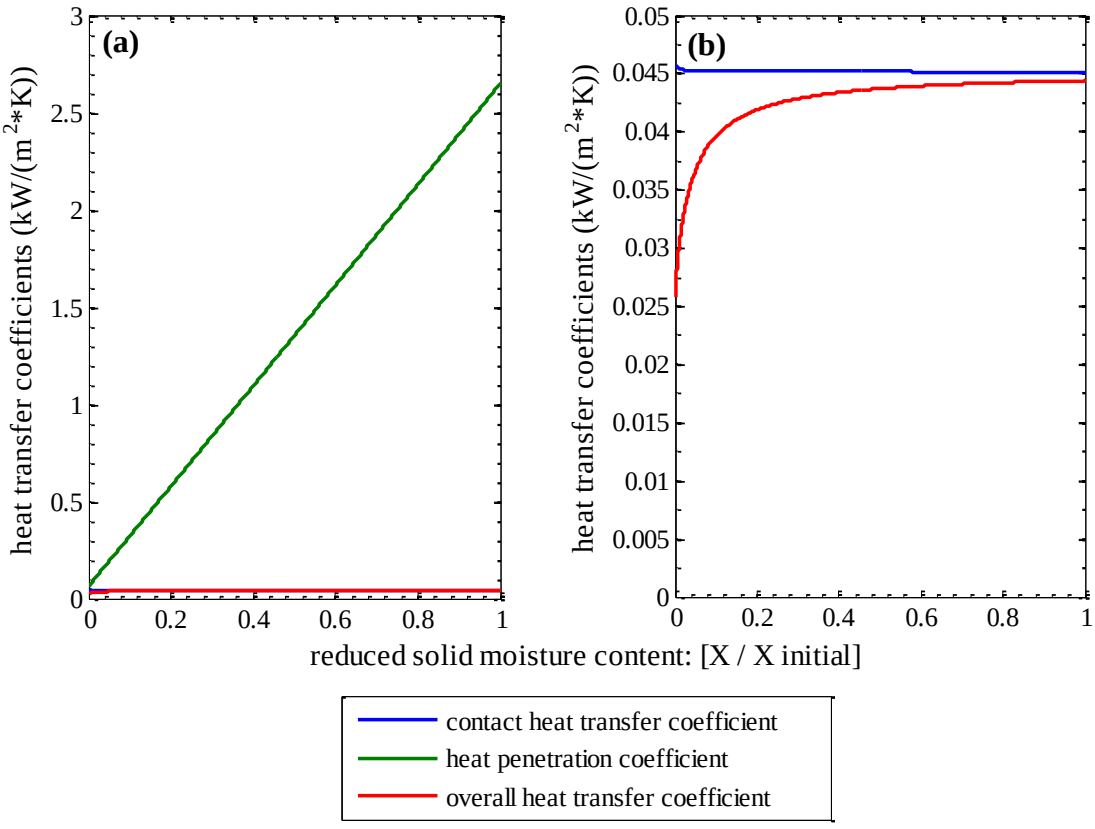

Figure 7.2. *(a) heat transfer coefficients (contact, penetration and overall heat transfer coefficient) during vacuum contact drying of agitated particulate material, as a function of reduced moisture content. Input data set: Sim. A.1. (b) zoom on the contact and overall heat transfer coefficients.*

[11] i.e. the temperature rise of the just dry particle above the saturation temperature.

In figure *7.2 (a)*, *heat penetration coefficient* shows a high value at the beginning of the process (above 100 times greater to contact heat transfer coefficient). Then, an almost linear decrease with the decrease of the moisture content is observed. This fall in the heat penetration coefficient (i.e. this increase of the bed heat transfer resistance) is due to the penetration of the drying front inside the bed. Anyhow the heat penetration resistance is greater than the contact one along the whole process.

Contact heat transfer coefficient, high-lined in figure *7.2 (b)* shown a constant value from the beginning of the process to the major part of it. Only for low relative moisture content (lower than 0.1), when the bed temperature rise up, the contact heat transfer coefficient shown a small increase due to radiation. Contact heat transfer is then the controlling heat transfer step along the whole process. The overall heat transfer coefficient is the results of the two heat transfer resistance in series. For this reason, it is every time lower than the lower of the two (contact coefficient), and it follows the decrease of the heat penetration coefficient.

Effective properties profiles

Effective bed density and bed specific heat capacity values are used constants in the simulations. On the other hand, the effective bed thermal conductivity is function of bed temperature. The effective bed thermal conductivity profile as function of relative moisture content of the bed is shown in figure *7.3*.

At the beginning of the process, when the moisture content is high (right side of the figure) the bed temperature is quite constant (figure *7.1*), and then the effective thermal conductivity is also constant. As the process going on, the bed temperature rise, and the effective bed thermal conductivity fall down mainly due to the effect of temperature on radiative heat transfer and on the mean free path of gas molecules.

Comparison with experimental data

A comparison between the simulation results and experimental data was carry out. Drying rate curves of contact drying of particulate pharmaceutical excipient (talc, indicated as *MgSi* and kaolin, indicated as *AlSi*) wetted by water, under vacuum, was found in literature (Schlünder & Mollekopf, 1984). In that work, drying rate curves of

different powder at several operating condition in three kind of contact dryer are presented.

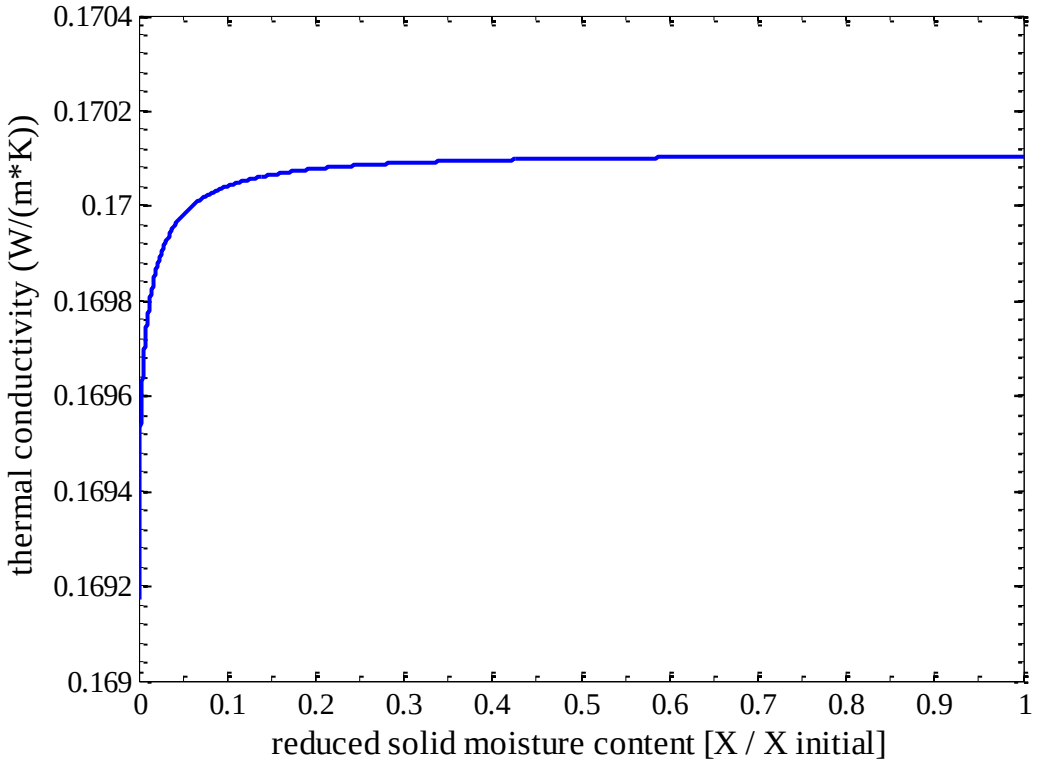

Figure 7.3. *Effective thermal conductivity of the particulate bed during vacuum contact drying of agitated material as a function of reduced moisture content. Input data set: Sim. A.1.*

Drying rate curves in disc dryer were choosen, and the program for vacuum contact drying of agitated beds was carry out in order to simulate the experimental set up of Schlünder and Mollekopf. For this purpose several experimental condition should be known, in order to know all the input data required by the program. Schlünder and Mollekopf work is not the only pubblication with the experimental drying rate curves, but is the one with most defined experimental condition.

Input data

Two input data were not provided in the Schlünder and Mollekopf work:

- Solid thermal conductivity;
- Bed porosity.

Value for both of them were found in literature. Talc thermal conductivity lies between 1.701 and 3.54 W/m*K (Gummnow & Sigalas 1988) in dependence of the thermal treatment of the powder. In the contact drying simulations this value was took as a "free value" inside the range, in order to fit the experimental curves. Regarding kaolin, the thermal conductivity value lies between 0,34 and 3,2 W/m*K (Michot, et.al. 2008) in dependence of thermal treatment of the powered. Also in this case the value was taken as a free parameter within the literature range.

Wall temperature

The effects of an increase of the heating wall temperature are analyzed in this section. In Table *1* of *Appendix D* there are all the fixed parameters used in the simulation as a input data. The simulated drying rate curve and the experimental point from literature (Schlünder & Mollekopf, 1984) are exposed in Figure *7.4*. A good agreement between simulated and experimental drying rate curves is shown.

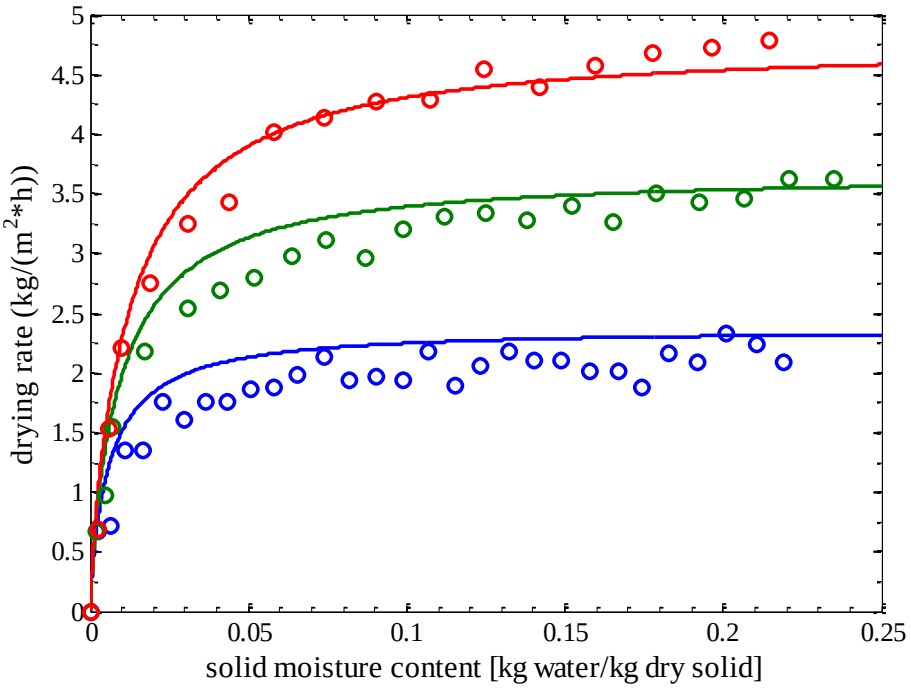

Figure 7.4. *Drying rate curves. Lines: simulation results of vacuum contact drying at different heating wall temperature. Blue line: Sim. A.1, wall temperature = 50.5°C. Green line: Sim. A.2, wall temperature = 70.6°C. Red line: Sim. A.3, wall temperature = 85.8°C . Dots: experimental data from (Schlünder & Mollekopf, 1984)*

About the effect of the wall temperature on the drying rate curves, an enhancement of the drying rate is observed with the wall temperature increase. The rising in the wall temperature produce a increase in the temperature gradient between heating wall and particle bed, that is the driving force to the heat transfer to the bed. Then with the rise up of the heat flux, a largest value of drying rate is obtained.

Pressure

The comparison between simulated and experimental drying rate curves at different pressure are exposed and a discussion about the sensitivity of the drying rate for a pressure variation are presented. The input data is in table *2* of *Appendix D*. The simulated drying rate curve and the experimental dots are shown in Figure *7.5* for three different pressure.

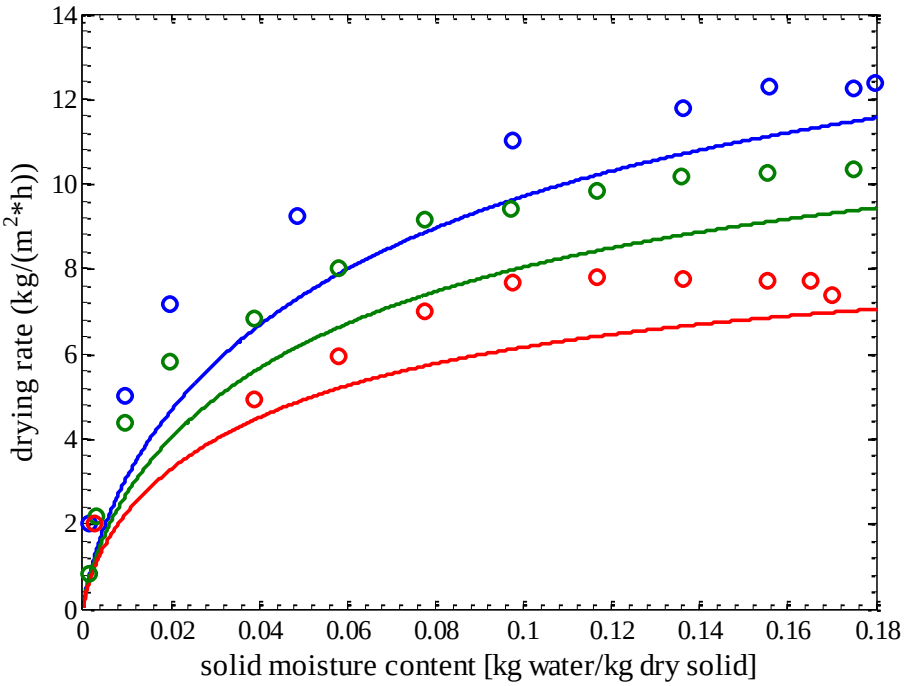

Figure 7.5. *Drying rate curves. Lines: simulation results of vacuum contact drying at different pressure. Blue line: Sim. B.1, pressure = 4500 Pa. Green line: Sim. B.2, pressure = 7000 Pa. Red line: Sim. B.3, pressure = 17500 Pa. Dots: experimental data from (Schlünder & Mollekopf, 1984)*

Figure *7.5* show a not good agreement, compared to previous case, between simulated and experimental data. All the three simulated drying curves are underestimated of the above same value. The reason of this behaviour is connected to the estimation of mixing

number. In order to confirm that, simulation of drying rate curves was carried out with mixing number as a free parameter, and a fitting on the experimental dots of figure *7.5* was done. The results is shown in figure *7.6*. With the best fitting mixing number, the program give a good estimation of the three experimental drying rate curves.

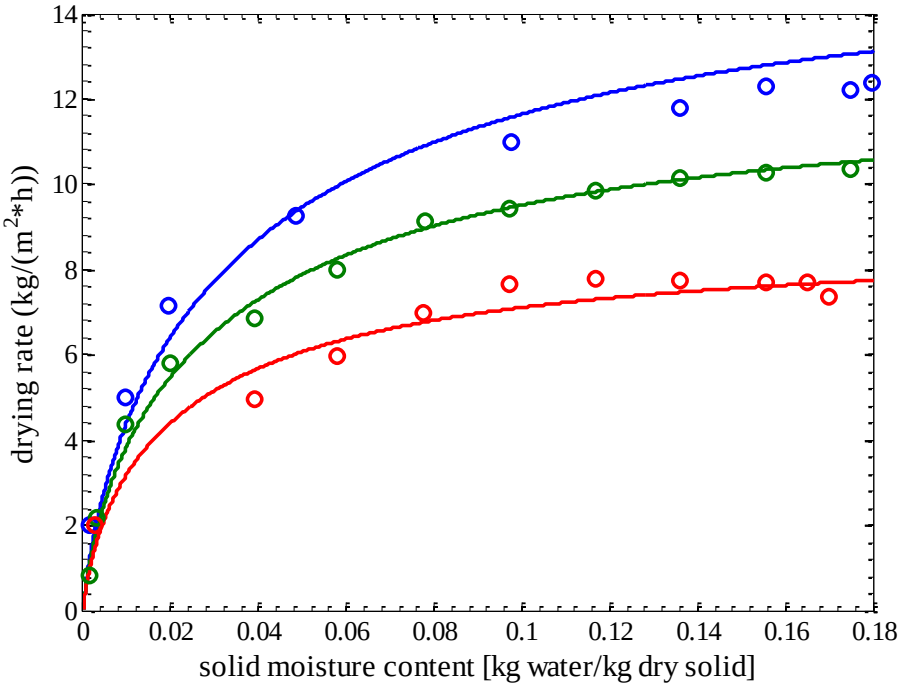

Figure 7.6. *Deying rate curves. Lines: best fitting simulation results of vacuum contact drying at different pressure, obtained with mixing number as a free parameter. Blue line: Sim. B.1, pressure = 4500 Pa. Green line: Sim. B.2, pressure = 7000 Pa. Red line: Sim. B.3, pressure = 17500 Pa. Dots: experimental data from (Schlünder & Mollekopf, 1984)*

In table *7.1* the mixing numbers calculated by eq.(14), are compared to the mixing numbers obtained by the best fitting on the experimental dots. The estimated mixing number is more than two time greater than the best fitting one.

Table 7.1. *Estimated value of mixing number by eq.(14) vs. best fitting mixing number.*

	Mixing number	
	Estimated value	Best fitting value
Sim. 1	16.4	7.5
Sim. 2	16.4	7.5
Sim. 3	16.4	7.5

About sensitivity analysis, pressure variation causes evident variation in the drying behaviour. The pressure effects is not direct, but is the variation of saturation temperature due to the pressure change that cause the different drying behaviour. In particular, when the pressure is fall down, the saturation temperature is fall down too. Then the bed temperature falls, and the temperature gradient between heating wall and bed rise. This phenomenon produce an increase of the drying rate with the pressure falls.

Stirring frequency

The comparison between simulated drying rate curves and experimental data at different stirring speed are presented in figure *7.7*. The input parameters used in the simulation are presented in table *3* of *Appendix D*. The experimental dots and the simulated curves are exposed in figure *7.5*.

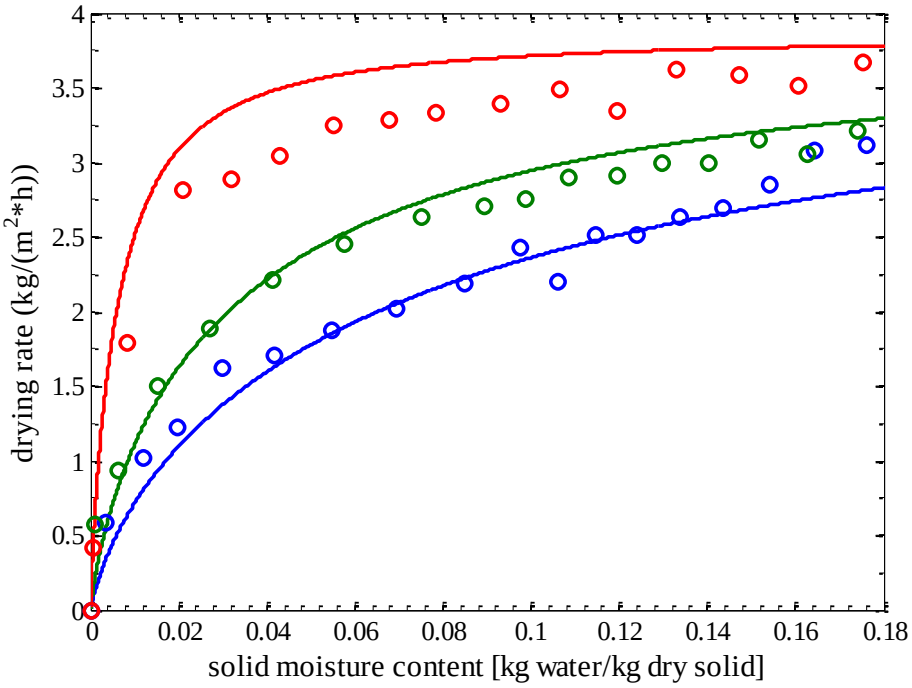

Figure 7.7. *Drying rate curves. Lines: simulation results of vacuum contact drying at different pressure. Blue line: Sim. C.1, stirring frequency = 0.2 rpm. Green line: Sim. C.2, pressure = 1 rpm. Red line: Sim. C.3, stirring frequency = 45 rpm. Dots: experimental data from (Schlünder & Mollekopf, 1984)*

The two simulations at 0.2 and 1 rpm show a good agreement with the experimental data. The simulation at 45 rpm show a small over-estimation of the drying rate. In this

case it is not imputable to a bad prevision of the mixing number. As exposed in table *7.2* the mixing number estimation is good, and in particular there is above the same deviation in all the three simulations.

Table 7.2. *Estimated value of mixing number by eq.(14) vs. best fitting mixing number.*

	Mixing number	
	Estimated value	Best fitting value
Sim. 1	2.21	2.00
Sim. 2	4.20	5.00
Sim. 3	19.3	22.5

The reason of the inconsistency between experimental and simulated value is then in another part of the model, related with the particle stirring. Almost certainly the problem is in the Penetration theory and is related to the high value of the stirring frequency.

In the Schlünder and Mollekopf work, where the experimental data were taken, some comparison between experimental data and simulated results obtained by implementation of Penetration theory are shown. In this work, all the drying rate curves simulated at stirring frequency equal or grather than *45 rpm*, show a deviation (under-esimation or over-estimantion) from the experimental data. Then, probably there is a limit in the penetration theory to describle the effect of the particle motion on the drying rate at hight stirring speed.

About the analysis of the profiles, the stirring frequency variation caused a variation in the contact time, and then in the value of the heat penetration coefficient. In particular, if the stirring frequency rise up, the bed mixing is improved, then the contact time become shorter and then the heat penetration coefficient rise up. Consequently an increase in the drying rate is observed.

7.2. Normal pressure contact drying

Simulation results

The simulation results i.e. the profile of effective properties, thermal coefficients, drying rate and temperature profiles are different in atmospheric contact drying respect to vacuum operations. All the results exposed in this section are referred to the input data of simulation *D.1* reported in *Appendix F*.

Drying rate and temperature profile

Drying rate profile of normal pressure contact drying with the input data of simulation *D.1* is exposed in figure *7.8*.

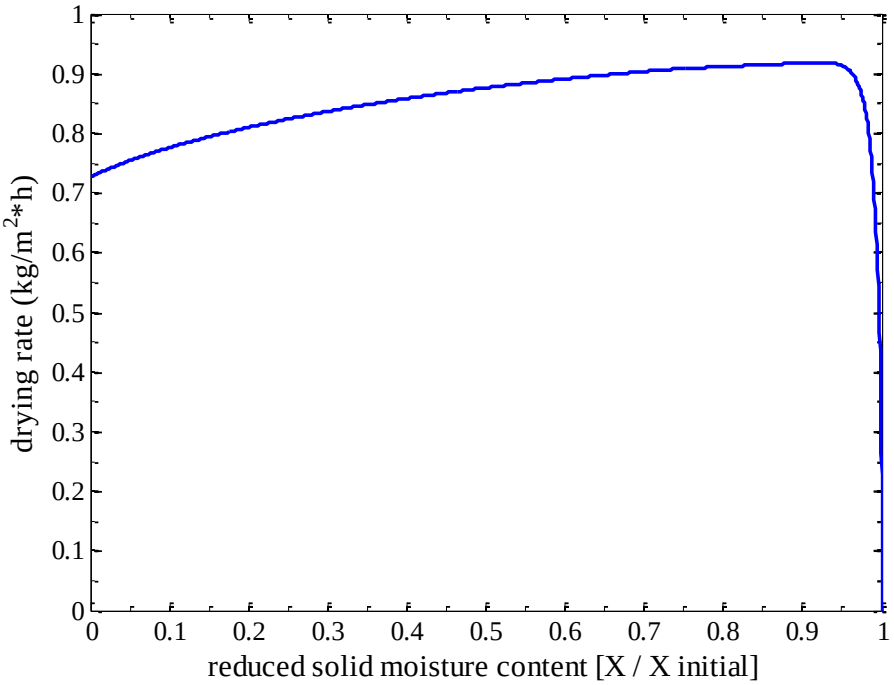

Figure 7.8. *Normalized drying rate curve during vacuum contact drying of agitated particulate material, as a function of reduced moisture content. Input data set: Sim. D.1.*

The shape of the drying rate profile is close to the heat penetration coefficient one (figure *7.11*). In particular the drying rate starts from zero, and then rise up immediately with the moisture content decrease, due to the bed temperature rise. Then, a slightly decrease starts due to the fall of the bed thermal conductivity. The influence of the heat

penetration profile in the drying rate behaviour is evident. As discussed more in detail later, the drying rate should go to zero for a totally dry bed (X = 0), but this not appeared in the simulations because of some transport phenomena are not taken into account in the used models.

In figure *7.9* three temperature profiles are shown: the temperature profile of the first particle layer in contact with the heating wall: T_H; the profile of the bulk temperature of the bed: T_b; and the temperature profile at the free surface of the bed in contact with the gas phase flow: T_o. For each one of the three temperature profiles, there is a fast rise up at the beginning of the process due to the effect of the heat transfer from the heating wall. After that, the three profiles carry on separately.

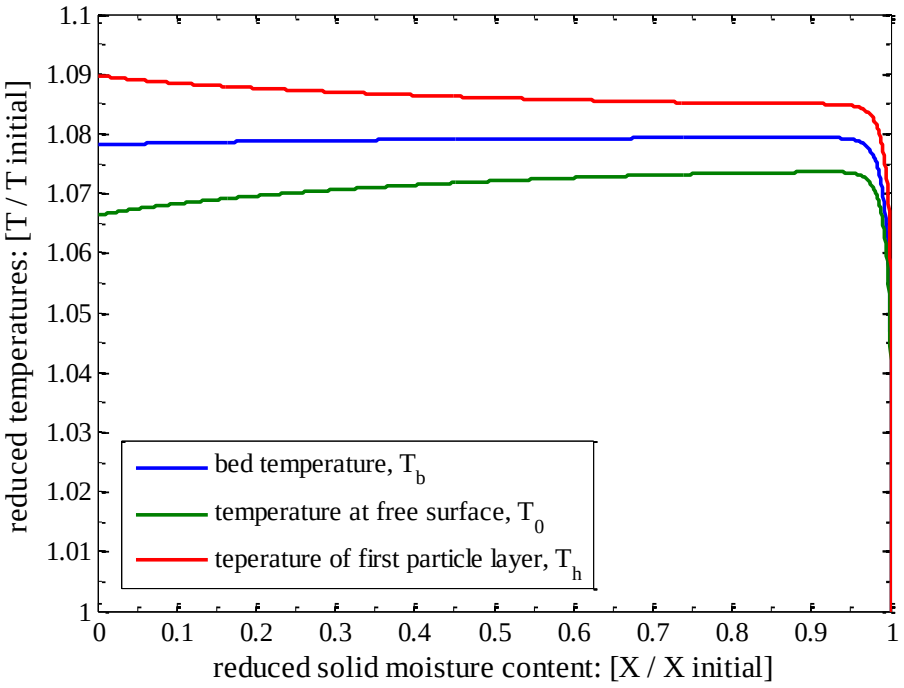

Figure 7.9. *Normalized bed temperatures during vacuum contact drying of agitated particulate material, as a function of reduced moisture content. Input data set: Sim. D.1.*

The highest temperature appear at the first particle layer in contact with the heating wall. Here the temperature continue with a slightly increase. The lowest temperature is at the top of the bed where the temperature slowly fall down, because of the loss of heat to the gas phase. The bulk bed temperature lies between the other two temperatures and shows a weak decrease at the end of the process due to the heat loss to the gas phase.

Heat transfer coefficients profiles during contact drying

In normal pressure contact drying modelling, three heat transfer coefficients are involved: contact, penetration and convective heat transfer coefficient[12]. The profiles of the heat transfer coefficients are shown in figure *7.10*.

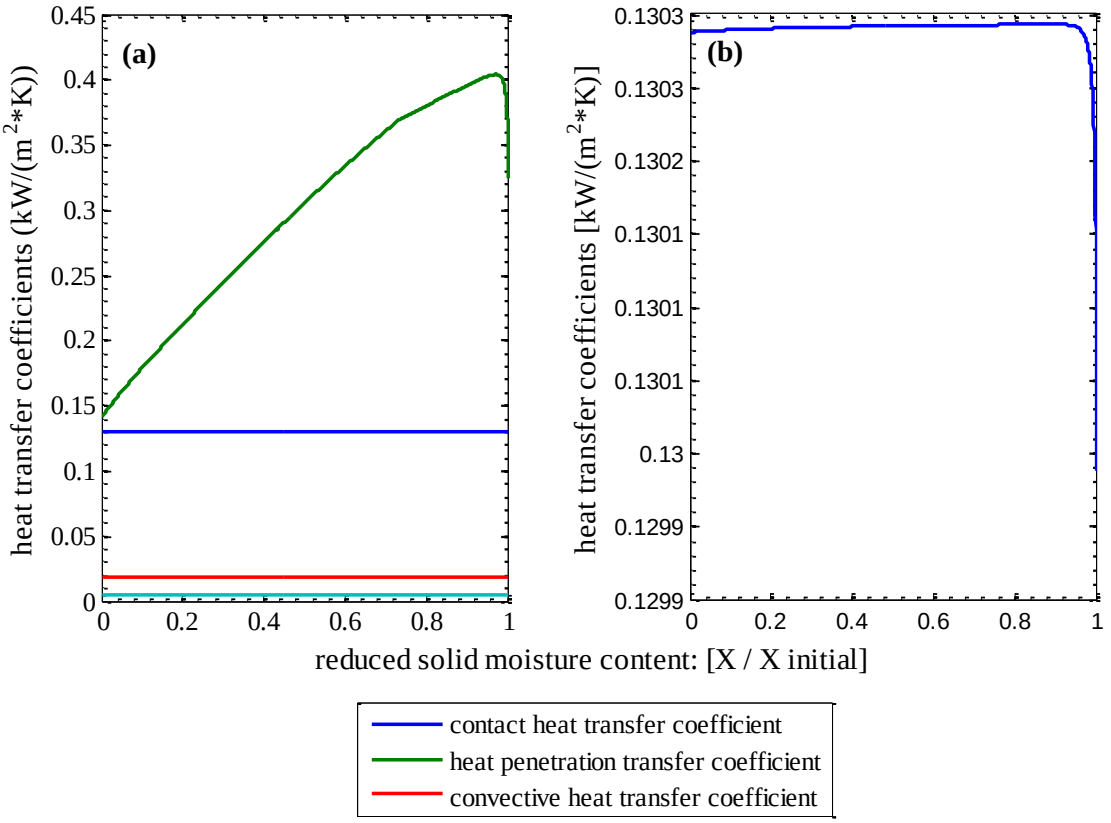

Figure 7.10. *(a) heat transfer coefficients (contact, heat penetration, convective and radiative heat transfer coefficients) during normal pressure contact drying of agitated particulate material, as a function of reduced moisture content. Input data set: Sim. D.1. (b) zoom on the contact heat transfer coefficient.*

The two coefficients (radiative and convective), for heat transfer from the free surface of the bed to the bulk of the gas phase, are practically constants during the process (*figure 7.10 (a)*). In particular, the convective heat transfer coefficient is around 4 times greater than the radiative one. The two heat transfer coefficients appeared in the model in parallel, then the radiative one could be neglected. The profile of the mass transfer

[12] "convective heat transfer coefficient" is referred to the coefficient for the heat transfer from the free surface of the bed to the inert gas flow.

coefficient from the bed surface to the gas phase is similar to the convective heat transfer coefficient by Lewis analogy, and then it is constant too.

Contact heat transfer coefficient is function of temperature and its profile shown a similarity to the bed temperature profile. The global variation of this heat transfer profile is anyway small, around 0.2% (figure *7.10 (b)*).

Much more larger is the global variation of the heat penetration coefficient. It is a function of temperature and moisture content of the bed. The more evident dependence in the profile is the moisture content one. In particular, the heat penetration coefficient is a function of the moisture content due to the effective bed conductivity dependence. Indeed, the shape of the heat penetration profile is similar to the shape of the effective bed thermal conductivity profile, that is shown in figure *7.11 (c)*. The global variation of the heat penetration coefficient is around 54% in this simulation, than the effect of the variation of the bed condition during the process have a clear influence on this parameter. Also in this case the value of the heat penetration coefficient is greater than the contact heat transfer coefficient, in particular at the beginning of the process. For this reason the controlling heat transfer phenomena is the contact heat transfer.

Effective properties profiles

In vacuum contact drying the effective properties are referred to a dry bed, and then they are fixed or lightly function of temperature as seen before. In normal pressure contact drying the effective properties are referred to a wet bed, and then all of them are function of temperature and moisture content. The profile during normal pressure contact drying of the three effective properties (bed density, bed specific heat capacity and bed thermal conductivity) are shown in figure *7.11*.

In figure *7.11 (a)* the bed density profile is shown. There is an initial bed density drop due to a temperature increase at the beginning of the process. After that, the bed density rise up, because the bed temperature become stable, and the liquid content of the bed decrease[13]. Anyhow the variation of the bed density is still low.

In figure *7.11 (b)* the bed specific heat capacity shown a linear decrease as the drying process going on. The liquid specific heat capacity is higher than the solid specific heat

[13] Since as the liquid density (around 1000 kg/m^3) is less than the solid density (2500 kg/m^3) a drop in the bed liquid content causes a bed density fall.

capacity, and then the falling of the moisture content produces a bed specific heat capacity reduction of around 2 times.

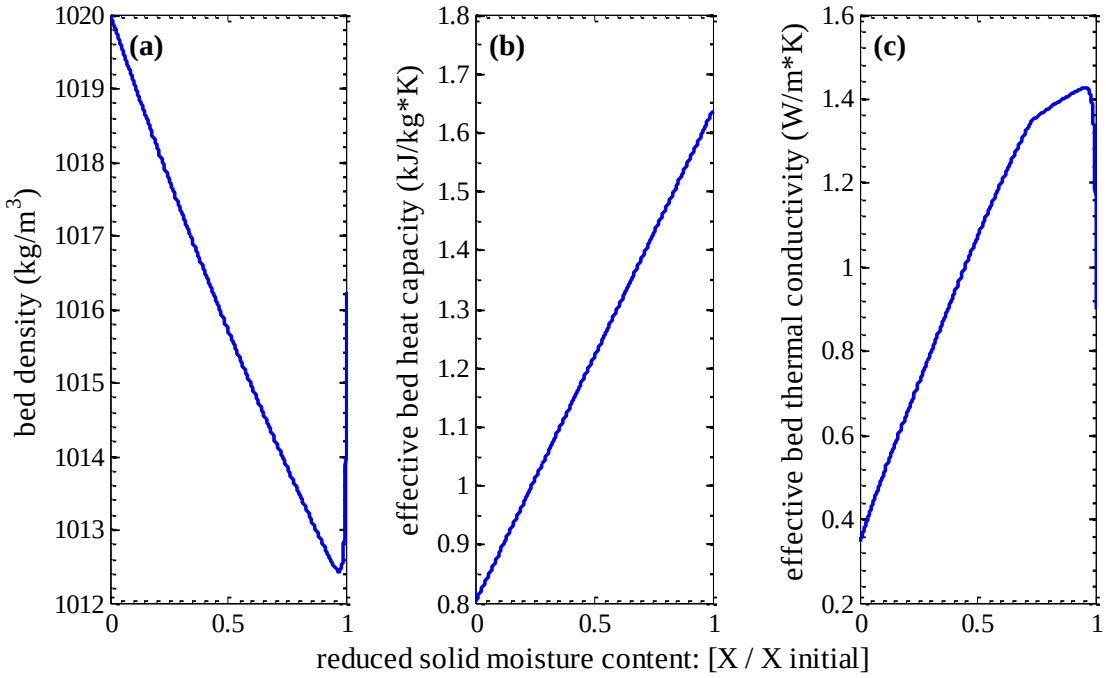

Figure 7.11. *Effective properties profiles of particulate agitated beds during normal pressure contact drying, as a function of reduced moisture content. (a) bed density. (b) bed specific heat capacity. (c) bed thermal conductivity. Input data set: Sim. D.1.*

The effective bed conductivity profile is shown in figure *7.11 (c)*. During the drying process, an initial fast increase is observed, due to the bed temperature rising. Then, the profile reach a maximum and after that, a falling down due to the moisture content drop starts[14]. In particular, during the bed thermal conductivity drop, two stages can be found, associated with two different slopes of drying rate curve. In the first one stage, the evaporation of the interparticle moisture (external moisture) occur, and the particle pore are still wet. The second stage start when the external moisture is totally evaporated, and the evaporation of the moisture inside the particle pore begins. In this phase the bed thermal conductivity fall faster. The global variation of bed thermal conductivity during the drying process in this case is around 70%.

[14] The presence of a liquid phase in the particle pore and in the interparticle gaps improve the heat transfer across the bed and then the effective bed thermal conductivity.

Comparison with experimental data

A comparison between the simulation results and experimental data from literature was carry out. The experimental data are about drying rate curves of contact drying of agitated particulate bed of kaolin, (indicated as *AlSi*) a pharmaceutical excipient, wetted with water, in presence of air at atmospheric pressure. The source of the experimental data is a work of Tsotsas and Schlünder (Tsotsas & Schlünder, 1986). Also in this case the Tsotsas and Schlünder work was choosen because the major part of the required information are avilable in the pubblication.

Input data

Some of the required input data for the program are precisely declared in Tsotsas and Schlünder work of 1986 about the experimental curves exposed, except the following values:

- Height of the bed;
- Solid hold up;
- Bed density;
- Initial solid moisture content;
- Gas phase moisture content;
- Gas velocity.

The height of the bed is not explicitly declared, but the value used in the simulation is estimated like 0.05 *m* from the geometrical proportion of the scheme presented in the paper, starting from the know diameter value. The solid hold up i.e. the mass dry of particulate solid inside the dryer is estimated form the dryer volume and the bed density. The other three value are more uncertain because there is no way to estimate it in the paper, and then common value from other experiments on disc dryer of the same author are used.

Wall temperature

For normal pressure contact drying of agitated beds, only one experimental set with different wall temperature are available in the used literature, then only this one parameter is analyzed. All the input data used in the simulation are exposed In table *4* of *Appendix F,*. In figure *7.12* the experimental dots and the simulation results are shown.

The results show in general, a good agreement between experimental and simulated data of normal pressure contact drying of stirred beds. A deviation of the simulation results, from the experimental dots, appeared for each one of the three simulation at the end of the process, for relative moisture content less than 0.1.

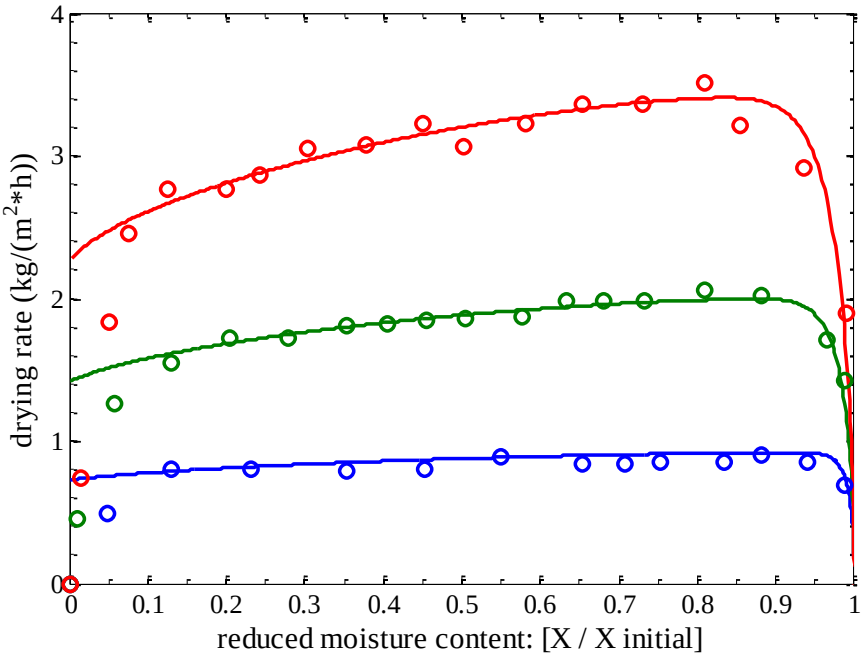

Figure 7.12. *Drying rate curves. Lines: simulation results of normal pressure contact drying at different heating wall temperature. Blue line: Sim. D.1, wall temperature = 50°C. Green line: Sim. D.2, wall temperature = 70°C. Red line: Sim. D.3, wall temperature = 90°C . Dots: experimental data from (Tsotsas & Schlünder, Contact drying of mechanically agitated particulate material in presence of inert gas, 1986)*

In particular, as the moisture content go to zero, the drying rate should go to zero too. In the simulation profiles this not happened. This behaviour was just noted by Toasts and Schlünder in the their work of 1986 where the experimental data were taken. Probably, this uncorrect description of the drying behaviour is due to the assumption of the used contact drying model. At the last sage of the drying process, whes the moisture content is low, the intraparticle heat and mass transfer resistances could became the controlling restances, but these phenomena were bot modelled.

About the influence of variation of wall temperature in normal pressure contact drying, an increase of drying rate is observed with a wall temperature rise up. The reason of this behaviour is connect with the vaporization mechanism. As the wall temperature rise up, the bed temperature rise up too, then the saturation temperature of the moisture inside

the bed increase. In this way the partial pressure gradient between the moisture in the bed and the moisture in the gas phase increase and then the moisture vaporization increase too.

Chapter 8

Conclusions

In this thesis work two programs for contact drying simulation of particulate beds, under two different operating condition: vacuum and normal pressure, were developed. The most suitable models available in literature was used to build up a complete contact drying model for each one of the two conditions. These contact drying models are based on *Penetration theory*, and the heat transfer coefficients, all the effective properties, the physical and thermodynamic properties, are evaluated by appropriate models.

Only initial conditions, operating conditions, geometrical data, type of substances, solid phase properties and the coefficients for mixing number evaluation, are required as input data. Then, the programs give a predictive estimation of the drying process.

The programs are based on a iteration cycle, where at each step, a short time period of the process is simulated. In every step, all the calculated coefficients and properties, are re-calculated at the actual bed temperature and moisture content, in order to give a realistic description of the profiles of these values during the process.

From the analysis of the results of the vacuum contact drying of stirred beds, the effective bed properties are constant, except effective bed thermal conductivity. It decreases during the process, but the total variation is probably negligible. The heat transfer from the heating wall to the first particle layer ("contact heat transfer") appears to be the controlling heat transfer step along the whole process. Then, the value of drying rate is strongly influenced by that. Instead, the decrease of the drying rate during the process, follow the decrease of the bulk penetration heat transfer coefficient.

The analysis of the results for inert gas contact drying show a not negligible variation of the effective bed properties during the process, in particular the bed thermal conductivity. The profile of this one has a large influence on the bulk penetration heat transfer profile. The effects of the two evaporation phases: external moisture and pore

moisture, is evident. The controlling heat transfer phenomenon is, also in this case, the contact heat transfer.

A validation of the developed programs was carry out by comparison of the simulation results with experimental data from literature, about pharmaceutical excipient. For vacuum contact drying of agitated beds, in general, good agreement was found in the drying rate value. Only two disagreements appeared. The first one at low vacuum (pressure > 4'500 Pa), due to a bad estimation of the mixing number. Then, an upper pressure limit for the validity of the used correlation at 4'500 Pa is suggest. The second one disagreement was found between simulated and experimental value at high stirring speed (> 45 rpm). In this case the problem is in the contact drying model. Penetration theory probably give a slightly uncorrected drying rate estimation for high particle mixing.

The comparison of simulated drying rate curve with experimental drying rate data at normal pressure show a good agreement for most of the drying process. Only for low moisture content (< 0.1% of the initial moisture content) a deviation appeared. That occurs because the internal heat and mass transfer phenomena are not modelled. If more accurate results are required at low moisture content the description of that phenomena is suggested.

In general, there was not the need to take into account the internal transfer resistances with the particles used in the simulation. Anyway the programs could be easily extended to the description of hygroscopic particles drying. The following further works about the programs could be done:

- coupling with solid phase models for heat and mass profiles inside the particle;
- extension to multi-component solvent mixtures.

Further studies to confirm the limitation in the application of the models emerged in this work should be done. Anyway, more accurate models for the prevision of the nixing number are required. Further studies are also suggest in order to extend the validation of the programs to:

- other pharmaceutical compound;
- particle wetted with other solvent;
- other contact drying equipment;

- temperature profiles validation;
- industrial scale validation.

With the developed programs, drying time, profile of drying rate, bed temperature can estimated in a predictive way with a satisfactory agreement with the analyzed experimental data. With the further works and validations proposed above, these programs could be a useful tool for design, analysis, optimization and control of industrial contact dryers.

Acknowledgments

First of all, I would like to express my gratitude to my thesis referent in Italy Prof. Paolo Canu at Padua University, for giving me the opportunity to carry out my Master Thesis work at Royal Institute of Technology - Stockholm, and for his support in this academic experience abroad.

I would like to express my gratitude to my supervisor, Prof. Joaquin Martinez, at Royal Institute of Technology - Stockholm, for the helpful guidance of my work.

I wish to express thank to Apolinar Picado for his fundamental support to this thesis, along all the work, from my first approach to drying modelling, to the review of the thesis.

I would like to thanks Elena for her helpful support, and all the friends who were close to me in this unforgettable experience in Sweden.

Nomenclature

A	heating wall area	[m^2]
Bi	Biot number	[-]
c_p	constant pressure specific heat capacity	[J/kg,K]
d	particle diameter	[m]
D	dryer diameter	[m]
$\mathcal{D}_{eff}$	effective diffusion coefficient	[m^2/s]
Fr	Froude number	[-]
g	gravitational constant	[m/s^2]
h	height of bed	[m]
Δh_{ev}	latent heat of vaporization	[J/kg]
Le	Lewis number	[-]
$\dot{m}$	drying rate	[kg/m,s^2]
$\dot{m}_{max}$	drying rate during constant rate period	[kg/m,s^2]
m_s	solid hold up	[kg]
MW	molar weight	[kg/kmol]
$\dot{n}$	molar drying rate	[kmol/ m,s^2]
N_{mix}	mixing number	[-]
p	partial pressure	[Pa]
P	pressure	[Pa]
Ph	reduced average solid moisture content	[-]
$\dot{q}$	heat flux	[J/m^2,s]
R	universal gas constant	[J/kmol,K]
t	time	[s]
t_R	contact time	[s]
t_{mix}	mixing time	[s]
T	temperature	[K]
v	gas velocity, or volume fraction	[m/s], [-]
x	length coordinate, or mass fraction	[m], [-]
X	solid phase moisture content (dry solid based)	[kg/kg]

Y	gas phase moisture content (dry gas based)	[kg/kg]
z	bed height coordinate	[m]
z_T	position of drying front	[m]

Greek letters

α	heat transfer coefficient	[W/m^2,K]
α_c	convective heat transfer coefficient	[W/m^2,K]
α_{dry}	overall heat transfer coefficient (dry bed)	[W/m^2,K]
α_r	radiative heat transfer coefficient	[W/m^2,K]
α_{sb}	heat penetration coefficient	[W/m^2,K]
$\alpha_{sb,dry}$	heat penetration coefficient (dry bed)	[W/m^2,K]
$\alpha_{sb,wet}$	heat penetration coefficient	[W/m^2,K]
α_{wet}	overall heat transfer coefficient (wet bed)	[W/m^2,K]
α_{ws}	contact heat transfer coefficient	[W/m^2,K]
β	mass transfer coefficient	[m/s]
ε	porosity	[-]
ζ	reduced instantaneous position of drying front	[-]
κ_{eff}	effective thermal diffusivity	[m^2/s]
λ	heat of vaporization	[J/kmol,s]
ρ	density	[kg/m^3]
τ_R	reduced penetration time	[-]

Subscripts

b	bulk of the bed
bed	referred to the particulate bed
b,m	bound moisture
$dry\ bed$	dry bed property (used in normal pressure drying modelling)
eff	effective property
g	of the gas phase
gas	in the gas phase
H	at first particle layer in contact with heating wall
in	inside

l	liquid phase, or "loss" if referred to $\dot{q}$
lat	latent
m	moisture
o	at the free surface above the bed
out	outside
p	particle
s	solid phase, or "saturation" if referred to T or P
sen	sensible
u,m	unbound moisture
w	at heating wall
$wet\ bed$	wet bed property (used in vacuum drying modelling)
0	initial

References

Aulton, M. E. (2007). *Pharmaceutics, the design and manufacture of medicines, Third Edition.* Churchill Livingstone, Elsevier.

Bauer, R. (1982). Effektive radiale Wärmeleitfahigkeit gasdurchströmter Schüttungen aus Partikeln unterschiedlicher From und Grössenverteilung. *VDI-Forschungsh. , 1*, 195-212.

Carslaw, H. S., & Jaeger, J. C. (1959). *Conduction of heat in solids, 2nd ed.* Oxford University Press.

Chen, X. D. (2007). Moisture diffusivity in food and biological materials. *Drying Technology , 25:7*, 1203-1213.

Crank, J. (1975). *The mathematics of diffusion.* Oxford: Clarendon press.

Cundall, P. A., & Strack, O. D. (1979). A discrete numerical model for granular assemblies. *Geotecnique , 29*, 47-65.

Farges, D., Hemati, M., Laguérie, C., Vachet, F., & Rousseaux, P. (1995). A new approach to contact drying modelling. *Drying Technology , 13*, 1317 - 1329.

Kohout, M. U., & Stepanek, F. (2007). Multi-scale analysis of vacuum contact drying. *Drying Technology , 25:7,* 1265-1273.

Kohout, M. U., Collier, A. P., & Stepanek, F. (2006). Mathematical modeling of solvent drying from a static particle bed. *Chem. Eng. Sci. , 61*, 3674-3685.

Krischer, O. (1963). *Die wissenschaftlichen Grundlagen der Trocknungstechnik, 2nd ed.* Springer-Verlag.

Martinez, J., & Setterwalla, F. (1991). Gas-phase controlled convective drying of solids wetted with multicomponent liquid mixtures. *Chem. Eng. Sci. , 46,9*, 2235-2252.

Metzger, T., Kwapinska, M., M., P., Saage, G., & Tsotsas, E. (2007). Modern modelling methods in drying. *Trans. Porous Med. , 66*, 103-210.

Michaud, A. P. (2008). Optimization of crystalline powders vacuum contact drying with intermittent stirring. *Chem. Eng. Res. Des. , 86*, 606 - 611.

Michaud, A., Peczalski, R., & Andrieu, J. (2007). Experimental studying and modeling of crystalline powders vacuum contact drying with intermittent stirring. *Drying Technology , 25:7*, 1163-1173.

Michaud, A., Peczalski, R., & Andrieu, J. (2008). Modeling of vacuum contact drying of crystalline powders packed beds. *Chem. Eng. Process. , 47*, 722-730.

Mollekopf, N. (1983). *Wärmeübertragung an mechanisch durchmischtes Schüttgut mit Wärmesenken in Kontaktapparaten.* Karlsruher Institut für Technologie, Dissertation.

Mujumdar, A. S. (2007). An overview of innovation in industrial drying: current status and R&D needs. *Transp. Porous. Med. , 66*, 3 - 18.

Mujumdar, A. S. (2007). *Handbook of industrial drying, 3rd ed.* CRC Press.

Reid, R. C., Prausnitz, J. M., & Poling, B. (1987). *Properties of gases and liquids, 4th ed.* McGraw-Hill.

Salangen, H. J. (2000). The need for fundamental research on drying as perceived by the European chemical industry. *Drying Technology , 18:7*, 1610-1640.

Schlünder, E. (1980). Contact Drying of Particulate Material Under Vacuum. *Developments in Drying* (pp. 184 - 193). Montreal: Mujumdar, A. S. .

Schlünder, E. U. (2004). Drying of porous material during the constant and the falling rate period: a critical review of existing hypotheses. *Drying Technology , 22* (6), 1517 - 1532.

Schlünder, E. U. (1981). *Einführung in die Wärmeübertragung, 3rd ed.* Vieweg-Verlag.

Schlünder, E. U. (1984). Heat transfer to packed and stirred beds from the surface of immersed bodies. *Chem. Eng. Process. , 18*, 31-53.

Schlünder, E. U. (1971). Wärmeübertragung an bewegte Kungelschüttungen bei kurzfirstigem Kontakt. *Chem. Ing. Technik , 43* (11), 651.

Schlünder, E. U., & Mollekopf, N. (1984). Vacuum contact drying of free flowing mechanically agitated particulate material. *Chem. Eng. Process. , 18*, 93-111.

Tórrez, N., & Martinez, J. (1994). Drying of sorghum by immersion in heated particulate medium. *9th International Drying Symposium.*

Tsotsas, E., & Martin, H. (1987). Thermal conductivity of packed beds: a review. *Chem. Eng. Process. , 22*, 19-37.

Tsotsas, E., & Schlünder, E. U. (1986). Contact drying of mechanically agitated particulate material in presence of inert gas. *Chem. Eng. Process. , 20*, 277-285.

Tsotsas, E., & Schlünder, E. U. (1986). Vacuum contact drying of free flowing mechanically agitated multigranular packing. *Chem. Eng. Process. , 20*, 339-249.

Tsotsas, E., & Schlünder, E. U. (1987). Vacuum contact drying of mechanically agitated beds: the influence of hygroscopic behavior in the drying rate curve. *Chem. Eng. Process. , 21*, 199-208.

Tsotsas, E., Kwapinska, M., & Saage, G. (2007). Modeling of contact dryiers. *Drying Technology , 25:7*, 1377-1391.

Villanueva, M., Martinez, J., & Gamero, R. (2006). Instant beans obtained from simultaneous process of drying and size reduction. *XXII IACChE.*

Wunschmann, J., & Schlünder, E. U. (1974). Heat transfer from heated plates to stagnant and agitated beds of spherical shaped granules under normal pressure and vacuum. *Int. Heat Transfer Conf., 5*, pp. 49 - 53. Tokyo.

Yan, J., Deng, W., Li, X., Wang, F., Chi, Y., Lu, S., et al. (2009). Experimental and theoretical study of agitated contact drying of sewage sludge under partial vacuum condition. *Drying Technology , 27:6*, 787-796.

Zehner, P. (1973). Experimentelle und theoretische Bestimmung der effektiven Wärmeleitfähigkeit durchströmter Kungelschuttungen bei mässigen und hohen Temperaturen. *VDI-Forschungsh. , 558.*

Appendix A

Estimation of contact heat transfer coefficient

Following the Schlünder model (Schlünder E. U., Heat transfer to packed and stirred beds from the surface of immersed bodies, 1984), the contact heat transfer coefficient can be estimated by:

$$\alpha_{ws} = \phi_A \, \alpha_{wp} + (1 - \phi_A) \frac{2 \, \frac{\lambda_G}{d}}{\sqrt{2} + 2 \frac{(l + \delta)}{d}} + \alpha_{rad} \tag{54}$$

Where ϕ_A is the plate surface coverage factor. The particle heat transfer coefficient is calculated by:

$$\alpha_{wp} = 4 \, \frac{\lambda_G}{d} \left[\left(1 + 2 \frac{(l + \delta)}{d} \right) \ln \left(1 + 2 \frac{d}{(l + \delta)} \right) - 1 \right] \tag{55}$$

Where δ is the surface roughness of the particles and l is the modified mean free path of the gas molecules and follows from:

$$l = 2 \frac{2 - \gamma}{\gamma} \sqrt{\frac{2\pi RT}{MW_G}} \frac{\lambda_G}{P \left(2 c_{p,G} - \frac{R}{MW_G} \right)} \tag{56}$$

Where γ is the accommodation coefficient, that is around 0.8 to 0.9 for normal gases at moderate temperature. In all the simulation is take equal to 0.8.

The heat transfer coefficient by radiation can be calculated from the linearized Stefan-Boltzmann law:

$$\alpha_{rad} = 4 \, C_{12} T^3 \tag{57}$$

C_{12} is a constant and σ is the black body radiation coefficient.

Appendix B

Penetration theory: detailed equations and derivation for penetration heat transfer coefficient for agitated beds

The heat flux from the heating surface to the particle bed $\dot{q}_0$, coincides with the heat flux at the heating surface calculated from the Fourier's low:

$$\dot{q}_0 = \dot{q}(z=0) = -\lambda_{bed}\left(\frac{\partial T}{\partial z}\right)_{z=0} \tag{58}$$

The heat penetration coefficient is defined as:

$$\alpha_{sb} = \frac{\dot{q}_0}{T_H - T_b}$$

Where T_H is the first particle layer (in contact with the hot surface) temperature and T_b is the bed temperature. Then, the heat penetration coefficient α_{sb} be calculated as:

$$\alpha_{sb} = -\frac{\lambda_{bed}\left(\frac{\partial T}{\partial z}\right)_{z=0}}{T_H - T_b} \tag{59}$$

Now, the value of the heat penetration coefficient of the partially wet bed during each contact period, can be calculated as the time-average of the heat penetration coefficient of eq. (57) through the contact time:

$$\alpha_{sb,wet} = -\frac{1}{t_R}\int_0^{t_R} \frac{\lambda_{bed}\,(\partial T/\partial z)_{z=0}}{T_H - T_b}\; dt \tag{60}$$

The value of $(\partial T/\partial z)_{z=0}$ is calculated in analytical way, by the solution of Fourier's equation from the heating surface to the instantaneous position of the drying front:

$$\rho\, c_p\, \frac{\partial T}{\partial t} = \lambda_{bed}\frac{\partial^2 T}{\partial z^2} \tag{61}$$

The set of two boundary condition and one time condition is:

$$z = 0 \rightarrow T = T_H \tag{62}$$

$$z = z_T \rightarrow T = T_b \tag{63}$$

$$\rho\, X\, \Delta h_v\, \frac{\partial z_T}{\partial t} = -\lambda_{bed} \frac{\partial T}{\partial z} \tag{64}$$

The analytical solution of the boundary value problem gives:

$$T - T_b = (T_H - T_b) \left[\frac{\operatorname{erf}\left(\frac{z}{2\sqrt{\kappa_{bed}\, t}} \right)}{\operatorname{erf} \zeta} \right] \tag{65}$$

Where $\kappa_{bed} = \left(\lambda/\rho\, c_p\right)_{bed}$ is the heat diffusivity of the bed. ζ is the *instantaneous reduced position of the drying front*, and is defined from de instantaneous position of de drying front as:

$$\zeta = \frac{z_T}{2\sqrt{\kappa_{bed}\, t}} \tag{66}$$

From the analytical solution of eq. (59) exposed in eq. (63) the integral of eq.(58) can be evaluated and that equation yields:

$$\alpha_{sb,wet} = \frac{2}{\sqrt{\pi}} \sqrt{\frac{\left(\lambda/\rho\, c_p\right)_{bed}}{t_R}}\, \frac{1}{\operatorname{erf} \zeta} \tag{67}$$

And in the limits of X going to zero, yields the heat transfer penetration coefficient of dry bed:

$$\alpha_{sb,dry} = \lim_{X \to 0} \alpha_{sb,wet} = \frac{2}{\sqrt{\pi}} \sqrt{\frac{\left(\lambda/\rho\, c_p\right)_{bed}}{t_R}} \tag{68}$$

Now, the penetration resistance of the bed (dry or wet) lies in series with the contact resistance. Then, the overall heat transfer resistance is the sum this two value.

In case of wet bed:

$$\frac{1}{\alpha_{wet}} = \frac{1}{\alpha_{ws}} + \frac{1}{\alpha_{sb,wet}} \tag{69}$$

And in case of dry bed:

$$\frac{1}{\alpha_{dry}} = \frac{1}{\alpha_{ws}} + \frac{1}{\alpha_{sb,dry}} \tag{70}$$

From the solution for $\alpha_{sb,wet}$ in eq. (65) an for $\alpha_{sb,dry}$ (66), the reduced heat transfer coefficient of wet $(\alpha_{wet}/\alpha_{ws})$ and dry bed $\left(\alpha_{dry}/\alpha_{ws}\right)$ can be calculated as follow:

$$\frac{\alpha_{wet}}{\alpha_{ws}} = \frac{1}{1 + \left(\frac{\alpha_{ws}}{\alpha_{dry}} - 1\right) \operatorname{erf} \zeta} \tag{71}$$

$$\frac{\alpha_{dry}}{\alpha_{ws}} = \frac{1}{1 + \frac{\sqrt{\pi}}{2}\sqrt{\tau_R}} \tag{72}$$

Where τ_R is the *reduced penetration time*, that is connect to the penetration time by the definition:

$$\tau_R = \frac{{\alpha_{ws}}^2}{\lambda\, \rho\, c_p} t_R \tag{73}$$

If α_{ws} is estimated following *Appendix A*, the heat penetration coefficient of wet and dry bed can be calculated, but the value of the two reduced value ζ and τ_R must be known.

The reduced position of the drying front can be calculate by iterative solution on the following equation:

$$\sqrt{\pi}\, \zeta \exp \zeta^2 \left[\left(\frac{\alpha_{ws}}{\alpha_{dry}} - 1\right) \operatorname{erf} \zeta + 1\right] = \frac{1}{Ph}\left(\frac{\alpha_{ws}}{\alpha_{dry}} - 1\right) \tag{74}$$

Ph is the *phase-change number* (also called as *reduced average moisture content of the bulk*) and is a measure of the intensity of the latent heat sink. It is defined as, and it can be calculated from:

$$Ph = \frac{X\, \Delta h_v}{c_p (T_w - T_s)} \tag{75}$$

Appendix C

Zehner - Bauer model for effective thermal conductivity

The equation for the effective bed thermal conductivity estimation, of a mono-disperse particulate bed proposed by Zehner (Zehner, 1973) and Bauer (Bauer, 1982), is show with some adaptation .

Three dimensionless thermal conductivity are defined:

$$k_p = \frac{\lambda_p}{\lambda_g} \qquad k_G = \frac{\lambda_D}{\lambda_g} \qquad k_{bed} = \frac{\lambda_{bed}}{\lambda_g} \tag{76}$$

Where λ_p is the particle thermal conductivity, λ_g is the gas thermal conductivity, λ_D is the thermal conductivity of gas phase in Knudsen regime inside the gas-filled gaps, λ_{bed} is the effective thermal conductivity of the bed.

The equation for the bed thermal conductivity k_{bed} is:

$$k_{bed} = \left(1 - \sqrt{1-\psi_A}\right)\phi_A \left[\left(\psi_A - 1 + \frac{1}{k_G}\right) + k_R\right] + \sqrt{1-\psi_A}[\phi_A k_P + (1-\psi_A)k_c] \tag{77}$$

Where ϕ_A is the surface coverage factor, ψ_A is the total void fraction of the bed and k_c is the conductivity of the core of the unit cell, and can be calculated by:

$$k_c = \frac{2}{N}\left\{\frac{B(k_P + k_R - 1)}{N^2 k_G k_P}\ln\frac{k_P + k_R}{B[k_G + (1-k_G)(k_P + k_G)]} + \frac{B+1}{2B}\left[\frac{k_R}{k_G} - B\left(1 + \frac{1-k_G}{k_G}\right)k_R\right] - \frac{B-1}{Nk_G}\right\} \tag{78}$$

Where N is:

$$N = \frac{1}{k_G}\left(1 + \frac{k_R - Bk_G}{k_P}\right) - B\left(\frac{1}{k_G} - 1\right)\left(1 + \frac{k_G}{k_P}\right) \tag{79}$$

The accommodation factor B can be calculated by the follow approximation:

$$B = C_f \left(\frac{1-\psi_A}{\psi_A}\right)^{\frac{10}{9}} \tag{80}$$

And the dimensionless thermal conductivity k_R can be calculated by:

$$k_R = \frac{\lambda_R}{\lambda_G} = \frac{4\,\sigma}{2/(\varepsilon-1)} T^3 \frac{d}{\lambda_G} \tag{81}$$

Where $\sigma = 5.67 \cdot 10^{-8}\ W/(m^2K^4)$ is the black body radiation coefficient and ε = 0.85 is the emissivity of the particle surface.

In this calculation appears ψ_A: volumetric moisture content of the particles:

$$\psi_A = \frac{\rho_P}{\rho_{liq}} X \tag{82}$$

During the firsts steps of the drying process the volumetric moisture content of the particle is probably greater than the pore volume of the particle. In this case the moisture content of the particle is set as a constant and equal to the pore volume, the excess water is outside the particle and then is not take in account in this calculation. When the calculated moisture content volume fall under the pore volume, the calculated value as take in account. This algorithms can be summarize by this mathematical representation:

$$\psi_A(X) = \begin{cases} if\ \psi_A(X) > \varepsilon_P\ \ then: \psi_A(X) = \varepsilon_P \\ if\ \psi_A(X) \leq \varepsilon_P\ \ then: \psi_A(X) = \ \psi_A(X) \end{cases} \tag{83}$$

Appendix D

Kischer model for effective thermal conductivity

Kischer model (Krischer, 1963) is used for the estimation of the wet particle, and macropore thermal conductivity in normal pressure contact drying. The equations of the model are reported below.

Wet particle thermal conductivity in Krischer model

The estimation of the porous wet particle thermal conductivity take in account the following thermal conductivity both in series and in parallel:

- Solid thermal conductivity
- Moisture thermal conductivity
- Thermal conductivity between wet particle pore wall
- Thermal conductivity between dry particle pore wall

A representation of the mixed distribution of the series/parallel resistances is reported below:

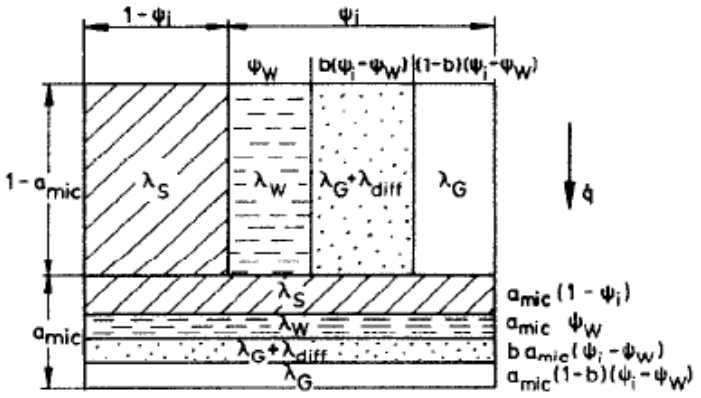

Figure A.1 *Graphical representation of distribution of the series/parallel resistances of the particles in Krischer model.*

The wet particle thermal conductivity is then:

$$\lambda_{P,wet} = \left(\frac{1 - a_{mic}}{\lambda_{P,ser}} + \frac{a_{mic}}{\lambda_{P,par}}\right)^{-1} \quad (84)$$

Where a_{mic} is the series/parallel arrangement factor of the resistance in the particle. In general a is defined as:

$$a = \frac{number\ of\ series\ resistances}{total\ nimber\ of\ resistances} \quad (85)$$

The parallel particle resistance $\lambda_{P,ser}$ can be calculated by:

$$\lambda_{P,par} = (1 - \psi_i)\lambda_s + \psi_w\lambda_w + b(\psi_i - \psi_w)(\lambda_{G,wet} + \lambda_{diff}) + (1 - b)(\psi_i - \psi_w)\lambda_{G,wet} \quad (86)$$

And the series particle resistance $\lambda_{P,ser}$ by:

$$\lambda_{P,ser} = \left[\frac{1 - \psi_i}{\lambda_s} + \frac{\psi_w}{\lambda_w} + \frac{b(\psi_i - \psi_w)}{\lambda_{G,wet} + \lambda_{diff}} + \frac{(1 - b)(\psi_i - \psi_w)}{\lambda_{G,wet}}\right]^{-1} \quad (87)$$

Where b is the air volume in the pore can be calculated by:

$$b = 1 - \left(1 - \frac{X}{X_0}\right)^9 \quad (88)$$

The effective thermal conductivity through diffusion of vapour λ_{diff} can be calculated by:

$$\lambda_{diff} = \frac{\delta}{R^2T^3}\frac{P_s}{1 - \frac{P_s}{P}}\Delta h^2 \quad (89)$$

And the thermal conductivity of a wet gas $\lambda_{G,wet}$ is:

$$\lambda_{G,wet} = \lambda_G(1 - y_{liq}) + \lambda_G y_{liq} \quad (90)$$

Where y_{liq} is the molar fraction of liquid in the gas phase. In this calculation appears ψ_w: volumetric moisture content of the particles:

$$\psi_w = \frac{\rho_P}{\rho_{liq}}X \quad (91)$$

During the firsts steps of the drying process the volumetric moisture content of the particle is probably greater than the pore volume of the particle. In this case the moisture content of the particle is set as a constant and equal to the pore volume, the excess water is outside the particle and then is not take in account in this calculation. When the calculated moisture content volume fall under the pore volume, the calculated

value as take in account. This algorithms can be summarize by this mathematical representation:

$$\psi_A(X) = \begin{cases} if\ \psi_w(X) > \varepsilon_P\ \ then: \psi_A(X) = \varepsilon_P \\ if\ \psi_w(X) \leq \varepsilon_P\ \ then: \psi_w(X) = \psi_w(X) \end{cases} \quad (92)$$

Wet gaps thermal conductivity in Krischer model

The gas gaps thermal conductivity is estimated by a combination of the following thermal conductivity both in series and in parallel:

- Thermal conductivity in the gaps between wet wall
- Thermal conductivity in the gaps between dry wall

A representation of the mixed distribution of the series/parallel resistances is reported below:

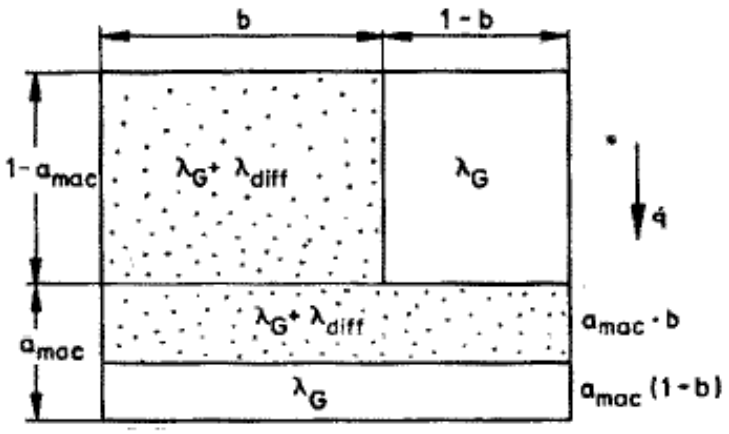

Figure A.2 *Graphical representation of distribution of the series/parallel resistances of the bed gaps in Krischer model.*

The thermal conductivity of the wet gaps between particles is then:

$$\lambda_{H,wet} = \left(\frac{1 - a_{mac}}{\lambda_{H,ser}} + \frac{a_{mac}}{\lambda_{H,par}}\right)^{-1} \quad (93)$$

Where a_{mic} is the series/parallel arrangement factor of resistance in the bed. The parallel gaps resistance $\lambda_{H,par}$ can be calculated by:

$$\lambda_{H,par} = b\left(\lambda_{G,wet} + \lambda_{diff}\right) + (1-b)\lambda_{G,wet} \tag{94}$$

And the series particle resistance $\lambda_{P,ser}$ by:

$$\lambda_{H,ser} = \left[\frac{b}{\lambda_{G,wet} + \lambda_{diff}} + \frac{(1-b)}{\lambda_{G,wet}}\right]^{-1} \tag{95}$$

Now $\lambda_{H,wet}$ and $\lambda_{H,wet}$ are the input data of Zehner – Bauer model as λ_G and λ_P.

Appendix E

Estimation of convective and radiative heat transfer coefficients

Convective heat transfer coefficient

The correlation to calculate the convective heat transfer coefficient α_c for forced convection around a solid bodies is exposed in (Schlünder E. U., Wärmeübertragung an bewegte Kungelschüttungen bei kurzfirstigem Kontakt, 1971) and summarized in (Schlünder & Mollekopf, Vacuum contact drying of free flowing mechanically agitated particulate material, 1984). The equation are reported below.

$$Nu = \frac{\alpha_c \, l}{k \, \lambda_G} \tag{96}$$

$$Nu = \left({Nu_{lam}}^2 + {Nu_{tur}}^2\right)^{1/2} \tag{97}$$

$$Nu_{lam} = 0.664 \, Pr^{1/3} \, {Re_{res}}^{1/2} \tag{98}$$

$$Nu_{tur} = \frac{0.37 \, Pr \, {Re_{res}}^{0.8}}{1 + 2.44(Pr^{2/3} - 1){Re_{res}}^{-0.1}} \tag{99}$$

$$Re_{res} = \left({Re_{forced}}^2 + \frac{Gr}{2.5}\right)^{1/2} \tag{100}$$

$$Re_{forced} = \frac{u \, l}{\nu_g} \tag{101}$$

$$Gr = \frac{l^3 g}{{\nu_g}^2} \frac{\rho_{g,\infty} - \rho_{g,0}}{\rho_{g,0}} \tag{102}$$

k is a correction factor. For disc dryer k = 1.5 (Tsotsas & Schlünder, Contact drying of mechanically agitated particulate material in presence of inert gas, 1986).

Radiative heat transfer coefficient

The radiative heat transfer coefficient is given by the following equation:

$$\alpha_{rad} = \frac{\varepsilon_p \, c_{p,s} \left(T_0^4 - T_g^4\right)}{T_0 - T_g} \tag{103}$$

Appendix F

Input data used in the simulations

Vacuum contact drying, agitated beds

Table 1. *Fixed input parameter used in the simulation of this section: Wall temperature.*

			Sim. A.1	Sim. A.2	Sim. A.3
Materials	Solid		*MgSi*	*MgSi*	*MgSi*
	Liquid		*water*	*water*	*water*
Initial values	moisture content	kg/kg	0.25	0.25	0.25
Operating parameters	Pressure	Pa	1600	1600	1600
	Wall temperature	°C	50.5	70.6	85.8
	Stirring frequency	rpm	15.4	15.4	15.4
	Solid hold up	kg	1	1	1
Solid phase properties	thermal conductivity	W/m*K	1.701÷3.54	1.701÷3.54	1.701÷3.54
	specific heat capacity	J/kg*K	800	800	800
Particle geometry	diameter	m	0.006	0.006	0.006
	roughness	μm	20	20	20
	Shape factor	-	1.25	1.25	1.25
Bed geometry	Bed diameter	m	0.24	0.24	0.24
	Bed density	kg/m^3	980	980	980
	Bed porosity	-	0.4	0.4	0.4
Time length of one calculation step		s	0.2*t_R	0.2*t_R	0.2*t_R

Table 2. *Fixed input parameter used in the simulation of this section: Pressure.*

			Sim. B.1	Sim. B.2	Sim. B.3
Materials	Solid		*AlSi*	*AlSi*	*AlSi*
	Liquid		*Water*	*Water*	*Water*
Initial values	moisture content	kg/kg	0.18	0.18	0.18
Operating parameters	Pressure	Pa	4500	7000	17500
	Wall temperature	°C	80	80	80
	Stirring frequency	rpm	30	30	30
	Solid hold up	kg	1	1	1
Solid phase properties	thermal conductivity	W/m*K	0,34÷3.2	0,34÷3.2	0,34÷3.2
	specific heat capacity	J/kg*K	800	800	800
Particle geometry	diameter	m	0.0011	0.0011	0.0011
	roughness	μm	2.5	2.5	2.5
	Shape factor	-	1.25	1.25	1.25
Bed geometry	Bed diameter	m	0.24	0.24	0.24
	Bed density	kg/m^3	1020	1020	1020
	Bed porosity	-	0.4	0.4	0.4
Time length of one calculation step		s	$0.05*t_R$	$0.05*t_R$	$0.05*t_R$

Table 3. *Fixed input parameter used in the simulation of this section: Stirring frequency.*

			Sim. C.1	Sim. C.2	Sim. C.3
Materials	Solid		*MgSi*	*MgSi*	*MgSi*
	Liquid		*Water*	*Water*	*Water*
Initial values	moisture content	kg/kg	0.25	0.25	0.25
Operating parameters	Pressure	Pa	190	190	190
	Wall temperature	°C	70.9	70.9	70.9
	Stirring frequency	rpm	0.2	1	45
	Solid hold up	kg	1	1	1
Solid phase properties	thermal conductivity	W/m*K	1.701	1.701	1.701
	specific heat capacity	J/kg*K	800	800	800
Particle geometry	diameter	m	0.006	0.006	0.006
	roughness	μm	20	20	20
	Shape factor	-	1.25	1.25	1.25
Bed geometry	Bed diameter	m	0.24	0.24	0.24
	Bed density	kg/m^3	980	980	980
	Bed porosity	-	0.4	0.4	0.4
Time length of one calculation step		s	$0.01*t_R$	$0.02*t_R$	$0.15*t_R$

Normal pressure contact drying, agitated beds

Table 4. *Fixed input parameter used in the simulation of this section: Wall temperature.*

			Sim. D.1	Sim. D.2	Sim. D.3
Materials	Solid		*AlSi*	*AlSi*	*AlSi*
	Liquid		*Water*	*Water*	*Water*
	Gas		*air*	*air*	*air*
Initial values	moisture content	kg/kg	0.18	0.18	0.18
	Bed temperature	°C	20	20	20
Operating parameters	Pressure	Pa	101325	101325	101325
	Wall temperature	°C	50	70	90
	Stirring frequency	rpm	63.0	60.0	60.4
	Solid hold up	kg	1.5	1.5	1.5
	Gas velocity	m/s	0.3	0.3	0.3
	Gas temperature	°C	40	40	40
	Gas abs. humidity	kg/kg	0.024	0.024	0.024
Solid phase properties	thermal conductivity	W/m*K	3.2	3.2	3.2
	specific heat capacity	J/kg*K	800	800	800
	Intrinsic density	Kg/m^3	2500	2500	2500
Particle geometry	diameter	m	0.004353	0.004353	0.004353
	roughness	µm	2.5	2.5	2.5
	Shape factor	-	1.25	1.25	1.25
	Particle porosity	-	0.375	0.375	0.375
	Micropore series/parallel arrangement factor	-	0.075	0.075	0.075
Bed geometry	Bed diameter	m	0.1	0.1	0.1
	Bed height	m	0.05	0.05	0.05
	Bed density	kg/m^3	1020	1020	1020
	Macropore series/parallel arrangement factor	-	0.20	0.20	0.20
Computational parameters	Number of steps	-	558	621	584
	Step time length	s	$5*t_R$	$5*t_R$	$5*t_R$

Appendix G

Vacuum contact drying simulation program

*fixed parameters declaration (*an example in table *1* of *Appendix F)*

contact time calculation

saturation temperature at operating pressure

initial variables

- bed moisture content = initial bed moisture content
- bed temperature = saturation temperature of liquid

physical property function of T

- Specific heat capacity of the liquid
- Liquid heat of vaporization

calculation of thermal coefficients

- average temperatures for the evaluation of heat transfer coefficients
- heat transfer coefficient by radiation
- contact heat transfer coefficient

maximum drying rate (constant period)

time variables

- total time length of the simulation
- time length of each iteration

CALCULATION CYCLE

- *Calculation of heat transfer coefficients*
  - heat penetration coefficient (dry bed)
  - overall dry heat transfer coefficient
  - Reduced average moisture content of the bulk
  - Reduced instantaneous position of drying front
  - heat penetration coefficient (wet bed)

  - overall wet heat transfer coefficient
- *heat fluxes*
  - heat flux at the hot surface (maximum)
  - heat flux at the drying front (minimum)
- *drying rate*
  - characteristic drying rate
  - drying rate (maximum value)
  - drying rate (minimum value)
- *results data saving*

INFORMATION FOR THE NEXT STEP

- *time step*
- *bed moisture content drop*
- *bed temperature rise*
- *Recalculation of physical property function of T*
  - Specific heat capacity of the liquid
  - mass heat of vaporization
- *Calculation of heat transfer coefficients*
  - average temperatures for the evaluation of heat transfer coefficients
  - heat transfer coefficient by radiation
  - contact heat transfer coefficient

END OF CYCLE

Appendix H

Normal pressure contact drying simulation program

*fixed parameters declaration (*an example in table *4* of *Appendix F)*

contact time calculation

moisture content of the gas phase (conversion to molar basis)

initial variables

- bed moisture content = initial bed moisture content
- bed temperature = initial sold temperature

physical property function of T

- Density of the liquid
- Mass and volume fraction of solid and liquid
- Specific heat capacity of the liquid
- Bed specific heat capacity
- Bed density
- density times specific heat capacity of the wet bed

calculation of heat transfer coefficients

- average temperatures for the evaluation of heat transfer coefficients
- heat penetration coefficient
- convective heat transfer coefficient
- heat transfer coefficient by radiation
- contact heat transfer coefficient

drying rate = 0

time variables

- total time length of the simulation
- time length of each iteration

CALCULATION CYCLE

- *iterative program at the free surface*
  - guess value for surface temperature
    - evaluation of physical property function of T
    - calculation of convective heat transfer coefficient
    - characteristic drying rate
    - calculation of drying rate
    - vaporization enthalpy calculations
    - calculation of radiative heat transfer coefficient
    - calculation of heat penetration coefficient
    - Evaluation of the heat balance residual
    - New guess temperature
  - Continue until convergence, Results: surface temperature, drying rate, latent heat flux, lost heat flux, output heat flux
- *iterative program at the hot surface*
  - guess value for the first particle layer temperature
    - evaluation of physical property function of T
    - calculation of radiative heat transfer coefficient
    - calculation of contact heat transfer coefficient
    - calculation of heat penetration coefficient
    - Evaluation of the heat balance residual
    - New guess temperature
  - Continue until convergence, Results: first layer temperature and input heat flux
- *calculation of sensible heat flux*
- *bed temperature rise*
- *bed moisture content drop*
- *recalculation of physical property function of T*
  - Density of the liquid
  - Mass and volume fraction of solid and liquid
  - Specific heat capacity of the liquid
  - Bed specific heat capacity
  - Bed density
  - density times specific heat capacity of the wet bed

- *calculation of heat transfer coefficients (only for data saving)*
  - average temperatures for the evaluation of heat transfer coefficients
  - heat penetration coefficient
  - heat transfer coefficient by radiation
  - contact heat transfer coefficient
- *time step*
- *results data saving*

END OF CYCLE